Slow Motion of Multiple Droplets in Arbitrary Three-Dimensional Configurations

Huan J. Keh and Yi K. Tseng
Dept. of Chemical Engineering, National Taiwan University, Taipei 106-17, Taiwan, Republic of China

This article presents a combined analytical-numerical study for the hydrodynamic interactions of an arbitrary finite cluster of spherical droplets at low Reynolds numbers. The droplets may differ in radius, in viscosity and in migration velocity. The theory developed is the most general solution to the mobility or resistance problem of slow motion of an assemblage of fluid spheres in a three-dimensional unbounded medium. Using a boundary collocation technique, the creeping flow equations are solved in the quasisteady situation, and the interaction effects among the droplets are evaluated for various cases. For the motion of two-droplet systems, our results for the droplet interaction parameters at all orientations and separation distances agree very well with the exact solutions obtained by using spherical bipolar coordinates or the asymptotic solutions obtained by using the connector algebra. The mobility parameters of linear chains of three droplets have been calculated, demonstrating that the existence of the third sphere can significantly affect the mobility of the other two spheres. The mobility results are also presented for the motion of chains containing up to 101 identical and equally spaced spheres, and the end effect exhibited by a chain of spheres can be found. Finally, our "exact" solutions for the hydrodynamic interaction between two fluid or solid spheres are used to find the effect of volume fractions of particles of each type on the mean settling velocities of the particles in a bounded suspension.

Introduction

The migration of particles or droplets through a viscous fluid at very small Reynolds numbers is of much interest in numerous technical applications, including the mechanics and rheology of suspensions or emulsions, sedimentation phenomena, meteorology, and colloidal studies. Problems of the slow motion of rigid particles have been treated extensively in the past. On the contrary, problems concerning fluid droplets caught less attention and are of a higher degree of difficulty due to the fact that the droplet is deformable and an additional flow field inside the droplet must be solved. The creeping-flow translation of a single fluid sphere of radius a in an unbounded, immiscible medium of viscosity η was first analyzed independently by Hadamard (1911) and Rybczynski (1911). Assuming continuous velocity and continuous tangential shearing stress across the interface of the phases in the absence of surface active agents, they found that the force exerted on the spherical droplet by the surrounding fluid is

$$\underline{F}^{(0)} = -6\pi\eta a \frac{3\eta^* + 2}{3\eta^* + 3} \underline{U}. \tag{1}$$

Here, $\underline{U}$ is the migration velocity of the droplet and η^* is the internal-to-external viscosity ratio. Since the fluid properties are arbitrary, Eq. 1 degenerates to the case of motion of a solid sphere (Stokes' law) when the viscosity of the particle becomes infinity and to the case of motion of a gas bubble when the viscosity approaches zero.

During the translation of a fluid sphere in a second, immiscible fluid, the interfacial stresses acting at the interface tend to deform it. If the motion is sufficiently slow or the droplet is sufficiently small, the droplet will in the first approximation be spherical. The problems associated with the

Correspondence concerning this article should be addressed to H. J. Keh.

shape of a droplet undergoing distortion, when inertial effects are no longer negligible, were discussed by Taylor and Acrivos (1964), and recently, by Dandy and Leal (1989). Even as early as in 1913, Boussinesq had criticized the theories advanced by Rybczynski and Hadamard arguing that, as the interface was undergoing continuous deformation, the state of stress at the interface should in general depend upon its rate of deformation (Happel and Brenner, 1983).

In most practical applications, particles or droplets are not isolated. So, it is important to determine if the presence of neighboring particles and/or boundaries significantly affects movement of the particles. Using spherical bipolar coordinates, Bart (1968) and Rushton and Davies (1973) examined the motion of a spherical droplet settling normal to a plane interface between two immiscible viscous fluids. This work is an extension of the analyses of Maude (1961) and Brenner (1961), who independently analyzed the fluid motion generated by a rigid sphere moving perpendicular to a solid plane surface or to a free surface plane. Wacholder and Weihs (1972) studied the motion of a fluid sphere through another fluid normal to a rigid or free plane surface; their calculations agree with the results obtained by Bart (1968) in these limits. Hetsroni et al. (1970) used a method of reflections to solve for the terminal settling velocity of a spherical droplet moving axially at an arbitrary radial location within a long circular tube filled with a viscous fluid. The wall effects experienced by a fluid sphere moving along the axis of a circular tube were also examined by using the reciprocal theorem (Brenner, 1971) and an approximative approach (Coutanceau and Thizon, 1981). Recently, the parallel motion of a droplet in a quiescent fluid between two parallel flat plates was studied by Shapira and Haber (1988) using the method of reflections.

On the other hand, Wacholder and Weihs (1972), Rushton and Davies (1973), and Haber et al. (1973) used the bispherical coordinate system to solve the problem of two arbitrary spherical droplets moving along their line of centers. This case is an extension of the pioneer treatment of Stimson and Jeffery (1926), who investigated the creeping motion of two solid spheres parallel to their line of centers with equal velocities. Wacholder and Weihs computed numerically the corrections to the Hadamard-Rybczynski law for the case of a pair of identical fluid spheres moving with equal velocity, while Rushton and Davies and Haber et al. obtained explicit expressions of the drag force on each droplet for the more general cases. The axisymmetric motion of two nearly touching droplets was studied by Davis et al. (1989) using lubrication approximations. Reed and Morrison (1974) employed tangent sphere coordinates to analyze the motion of two undeformed fluid spheres in apparent contact translating along their line of centers. In the limit of infinite internal viscosity, their calculations agree with the results of Cooley and O'Neill (1969) for the motion of a doublet of rigid spheres. Examples of streamline patterns for the axisymmetric motion of two fluid spheres and for the motion of a spherical droplet normal to a plane surface were provided by Rushton and Davies (1978).

For the slow motion of two spherical droplets in an arbitrary configuration, Hetsroni and Haber (1978) used the method of reflections to obtain the droplet-interaction solutions as series in a_1/r_{12} and a_2/r_{12} up to $O(r_{12}^{-5})$, where a_1 and a_2 are the radii of the droplets and r_{12} is their center-to-center distance. Using the so-called connector algebra, Geigenmuller and Mazur (1986) extended these solutions to $O(r_{12}^{-7})$ for the case of two identical drops. Recently, it was reported (Kim and Karrila, 1991) that the transverse motion of two identical spherical drops was solved by using a boundary-collocation method and the numerical results were in good agreement with other methods. The axisymmetric and transverse motions of two unequal drops were also examined by Fuentes et al. (1988, 1989) based on image solutions.

For concentrated dispersions, the interactions among multiple droplets can be important. The purpose of the present work is to investigate the slow motion of multiple fluid spheres in an arbitrary configuration. The droplets may differ in radius, in viscosity and in migration velocity. The creeping flow equations applicable to the system are solved by using a multipole collocation technique (Hassonjee et al., 1988) and the droplet interaction parameters are obtained with good convergence for various cases. For the simple case of movement of two spheres, our numerical calculations for the droplet interactions show excellent agreement with the exact solutions for the axisymmetric case obtained by using the bipolar coordinate system (Haber et al., 1973) and with the asymptotic solutions derived by Geigenmuller and Mazur (1986) or Hetsroni and Haber (1978). The complete collocation results for the hydrodynamic interactions between pairs of droplets are also employed to evaluate the average settling velocity in a bounded suspension of small droplets.

Analysis for Multiple Droplets

We consider the slow motion of N fluid droplets in an unbounded, immiscible fluid in an arbitrary three-dimensional configuration as shown in Figure 1. The droplets are assumed to be small enough so that interfacial tension maintains their spherical shape. It is also assumed that there is no coalescence and Marangoni stresses are not important. For convenience, the rectangular coordinate system (x, y, z) is established such that the center of the first sphere is at the origin. The position of the center of droplet i is represented by coordinates $(b_i, c_i,$

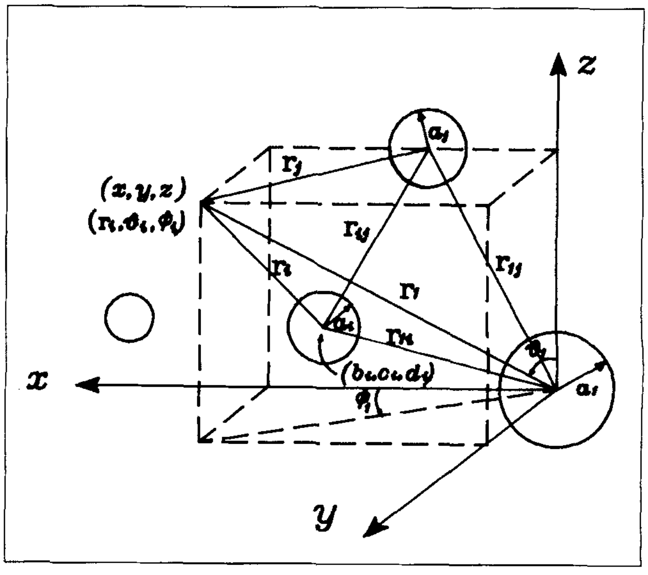

Figure 1. Geometric sketch of the slow motion of multiple spheres.

d_i), and we have set $b_1 = c_1 = d_1 = 0$. The droplets may be formed from different fluids and have unequal radii. Our purpose here is to determine the correction to Eq. 1 for the motion of each droplet due to the presence of the other ones in proximity.

Fluid velocity distribution

Assume that the Reynolds numbers are small and the problem can be viewed quasisteady. Hence, the fluid velocity inside and outside the droplets is governed by the Stokes equations,

$$\eta \nabla^2 \underline{v} - \nabla p = \underline{0} \tag{2a}$$

$$\nabla \cdot \underline{v} = 0 \tag{2b}$$

$$\eta_i \nabla^2 \underline{v}_i - \nabla p_i = \underline{0} \tag{2c}$$

$$\nabla \cdot \underline{v}_i = 0 \tag{2d}$$

for $i = 1, 2, \ldots$, or N. Here, $\underline{v}_i(\underline{x})$ and $\underline{v}(\underline{x})$ are the velocity fields for the flow inside droplet i and for the external flow respectively, $p_i(\underline{x})$ and $p(\underline{x})$ are the corresponding pressure distributions, and η_i and η are the corresponding viscosity coefficients. The boundary conditions for the fluid velocity at the droplet interfaces and at infinity are

$$r_i = a_i: \quad \underline{v} = \underline{v}_i \tag{3a}$$

$$\underline{e}_{ri} \cdot (\underline{v} - \underline{U}_i) = 0 \tag{3b}$$

$$(\underline{\underline{I}} - \underline{e}_{ri}\underline{e}_{ri})\underline{e}_{ri} : (\underline{\underline{\tau}} - \underline{\underline{\tau}}_i) = \underline{0} \tag{3c}$$

$$(x^2 + y^2 + z^2)^{1/2} \to \infty: \quad \underline{v} \to \underline{0} \tag{3d}$$

for $i = 1, 2, \ldots$, or N. Here, a_i is the radius of droplet i; (r_i, θ_i, ϕ_i) are the spherical coordinates measured from the center of droplet i; $\underline{e}_{ri}$ is the radial unit vector in the spherical coordinates; $\underline{\underline{I}}$ is the unit dyadic; $\underline{U}_i$, equal to $U_{ix}\underline{e}_x + U_{iy}\underline{e}_y + U_{iz}\underline{e}_z$, is the translational velocity of droplet i. The deviatoric stress tensors for the external flow and the flow inside droplet i can be expressed as

$$\underline{\underline{\tau}} = \eta[\nabla \underline{v} + (\nabla \underline{v})^T] \tag{4a}$$

and

$$\underline{\underline{\tau}}_i = \eta_i[\nabla \underline{v}_i + (\nabla \underline{v}_i)^T], \tag{4b}$$

respectively. The normal components of the normal stress vectors at the interface of droplet i have a discontinuity which is proportional to the surface tension γ_i. Presently we shall assume that the droplets are spherical (which implies that capillary numbers $\eta U_i/\gamma_i$ are much less than unity), and will not use this boundary condition.

The general solution to Eqs. 2 is

$$\underline{v} = \sum_{j=1}^{N} \sum_{n=1}^{\infty} [\nabla \times (\underline{r}_j \chi_{-n-1}^{(j)}) + \nabla \phi_{-n-1}^{(j)} - \frac{n-2}{2\eta n(2n-1)} r_j^2 \nabla p_{-n-1}^{(j)} + \frac{n+1}{\eta n(2n-1)} \underline{r}_j p_{-n-1}^{(j)}] \tag{5a}$$

$$\underline{v}_i = \sum_{n=1}^{\infty} [\nabla \times (\underline{r}_i \chi_n^{(i)}) + \nabla \phi_n^{(i)} + \frac{n+3}{2\eta_i(n+1)(2n+3)} r_i^2 \nabla p_n^{(i)} - \frac{n}{\eta_i(n+1)(2n+3)} \underline{r}_i p_n^{(i)}] \tag{5b}$$

where $\chi_n^{(i)}$, $\phi_n^{(i)}$ and $p_n^{(i)}$ are solid spherical harmonic functions of order n which depend on the spherical coordinates (r_i, θ_i, ϕ_i) originating at the center of droplet i and $\underline{r}_i = r_i \underline{e}_{ri}$. These harmonic functions can be expressed as

$$\begin{bmatrix} \chi_{-n-1}^{(j)} \\ \phi_{-n-1}^{(j)} \\ p_{-n-1}^{(j)} \end{bmatrix} = r_j^{-n-1} \sum_{m=0}^{n} P_n^m(\mu_j) \left\{ \begin{bmatrix} A_{jmn} \\ C_{jmn} \\ E_{jmn} \end{bmatrix} \cos(m\phi_j) + \begin{bmatrix} B_{jmn} \\ D_{jmn} \\ F_{jmn} \end{bmatrix} \sin(m\phi_j) \right\} \tag{6a}$$

$$\begin{bmatrix} \chi_n^{(i)} \\ \phi_n^{(i)} \\ p_n^{(i)} \end{bmatrix} = r_i^n \sum_{m=0}^{n} P_n^m(\mu_i) \left\{ \begin{bmatrix} \overline{A}_{imn} \\ \overline{C}_{imn} \\ \overline{E}_{imn} \end{bmatrix} \cos(m\phi_i) + \begin{bmatrix} \overline{B}_{imn} \\ \overline{D}_{imn} \\ \overline{F}_{imn} \end{bmatrix} \sin(m\phi_i) \right\} \tag{6b}$$

where P_n^m is the associated Legendre function of order m and degree n and μ_i is used to denote $\cos\theta_i$ for brevity. The requirement of finite fluid velocity in the interior of each droplet and the boundary condition Eq. 3d are immediately satisfied by a solution of this form. The unknown coefficients A_{jmn}, B_{jmn}, $\ldots$, F_{jmn} and $\overline{A}_{imn}$, $\overline{B}_{imn}$, $\ldots$, $\overline{F}_{imn}$ are to be determined using the boundary conditions at the droplet interfaces. In the construction of solution Eqs. 5, the superposition of Lamb's general solution (Happel and Brenner, 1983) to Eqs. 2 as written from N different origins can be utilized owing to the linearity of the governing equations.

In order to express the external velocity field Eq. 5a in terms of a single coordinate system, it is necessary to perform a transformation of coordinates. The coordinates (r_j, μ_j, ϕ_j) of an arbitrary position relative to the jth sphere are related to the coordinates (r_i, μ_i, ϕ_i) of the position relative to the ith sphere via the formulae

$$r_j^2 = [r_i(1-\mu_i^2)^{1/2}\cos\phi_i + b_{ij}]^2 + [r_i(1-\mu_i^2)^{1/2}\sin\phi_i + c_{ij}]^2 + (r_i\mu_i + d_{ij})^2 \tag{7a}$$

$$\mu_j = (r_i\mu_i + d_{ij})\{[r_i(1-\mu_i^2)^{1/2}\cos\phi_i + b_{ij}]^2 + [r_i(1-\mu_i^2)^{1/2}\sin\phi_i + c_{ij}]^2 + (r_i\mu_i + d_{ij})^2\}^{-1/2} \tag{7b}$$

$$\tan\phi_j = [r_i(1-\mu_i^2)^{1/2}\sin\phi_i + c_{ij}]/[r_i(1-\mu_i^2)^{1/2}\cos\phi_i + b_{ij}], \tag{7c}$$

where $b_{ij} = b_i - b_j$, $c_{ij} = c_i - c_j$ and $d_{ij} = d_i - d_j$. Caution must be taken in the use of Eq. 7c to ensure that the value of ϕ_j lies in the appropriate quadrant. The unit vectors of the jth and ith spherical coordinate systems are related by the matrix equation

$$\begin{pmatrix} \underline{e}_{rj} \\ \underline{e}_{\theta j} \\ \underline{e}_{\phi j} \end{pmatrix} = \begin{pmatrix} f_{ji}^{(1)} & f_{ji}^{(2)} & f_{ji}^{(3)} \\ f_{ji}^{(4)} & f_{ji}^{(5)} & f_{ji}^{(6)} \\ f_{ji}^{(7)} & f_{ji}^{(8)} & f_{ji}^{(9)} \end{pmatrix} \begin{pmatrix} \underline{e}_{ri} \\ \underline{e}_{\theta i} \\ \underline{e}_{\phi i} \end{pmatrix} \tag{8}$$

where

$$f_{ji}^{(1)} = (1-\mu_j^2)^{1/2}(1-\mu_i^2)^{1/2}\cos(\phi_j-\phi_i) + \mu_j\mu_i \tag{9a}$$

$$f_{ji}^{(2)} = (1-\mu_j^2)^{1/2}\mu_i\cos(\phi_j-\phi_i) - \mu_j(1-\mu_i^2)^{1/2} \tag{9b}$$

$$f_{ji}^{(3)} = (1-\mu_j^2)^{1/2}\sin(\phi_j-\phi_i) \tag{9c}$$

$$f_{ji}^{(4)} = (1-\mu_i^2)^{1/2}\mu_j\cos(\phi_j-\phi_i) - \mu_i(1-\mu_j^2)^{1/2} \tag{9d}$$

$$f_{ji}^{(5)} = \mu_j\mu_i\cos(\phi_j-\phi_i) + (1-\mu_j^2)^{1/2}(1-\mu_i^2)^{1/2} \tag{9e}$$

$$f_{ji}^{(6)} = \mu_j\sin(\phi_j-\phi_i) \tag{9f}$$

$$f_{ji}^{(7)} = -(1-\mu_i^2)^{1/2}\sin(\phi_j-\phi_i) \tag{9g}$$

$$f_{ji}^{(8)} = -\mu_i\sin(\phi_j-\phi_i) \tag{9h}$$

$$f_{ji}^{(9)} = \cos(\phi_j-\phi_i). \tag{9i}$$

In Eqs. 9 the variables μ_j and ϕ_j are associated to the coordinates r_i, μ_i and ϕ_i by Eqs. 7b and 7c.

Substituting Eqs. 6 into Eqs. 5 and applying Eqs. 7 to 9 for the coordinate transformation yield the expression for the fluid velocity field in terms of the spherical coordinates measured from the center of the ith droplet,

$$\underline{v} = v_r(r_i,\theta_i,\phi_i)\underline{e}_{ri} + v_\theta(r_i,\theta_i,\phi_i)\underline{e}_{\theta i} + v_\phi(r_i,\theta_i,\phi_i)\underline{e}_{\phi i} \tag{10a}$$

$$\underline{v}_i = v_{ri}(r_i,\theta_i,\phi_i)\underline{e}_{ri} + v_{\theta i}(r_i,\theta_i,\phi_i)\underline{e}_{\theta i} + v_{\phi i}(r_i,\theta_i,\phi_i)\underline{e}_{\phi i} \tag{10b}$$

where

$$v_{ri} = \sum_{n=1}^{\infty}\sum_{m=0}^{n}\Big\{nr_i^{n-1}P_n^m(\mu_i)[\overline{C}_{imn}\cos(m\phi_i) + \overline{D}_{imn}\sin(m\phi_i)] + \frac{n}{2\eta_i(2n+3)}r_i^{n+1}P_n^m(\mu_i)[\overline{E}_{imn}\cos(m\phi_i) + \overline{F}_{imn}\sin(m\phi_i)]\Big\} \tag{11a}$$

$$v_{\theta i} = \sum_{n=1}^{\infty}\sum_{m=0}^{n}\Big\{-mr_i^nP_n^m(\mu_i)(1-\mu_i^2)^{-1/2}\times[\overline{A}_{imn}\sin(m\phi_i) - \overline{B}_{imn}\cos(m\phi_i)] - r_i^{n-1}(1-\mu_i^2)^{1/2}\frac{dP_n^m(\mu_i)}{d\mu_i}[\overline{C}_{imn}\cos(m\phi_i) + \overline{D}_{imn}\sin(m\phi_i)] - \frac{(n+3)}{2\eta_i(n+1)(2n+3)}r_i^{n+1}(1-\mu_i^2)^{1/2}\frac{dP_n^m(\mu_i)}{d\mu_i}[\overline{E}_{imn}\cos(m\phi_i) + \overline{F}_{imn}\sin(m\phi_i)]\Big\} \tag{11b}$$

$$v_{\phi i} = \sum_{n=1}^{\infty}\sum_{m=0}^{n}\Big\{r_i^n(1-\mu_i^2)^{1/2}\frac{dP_n^m(\mu_i)}{d\mu_i}\times[\overline{A}_{imn}\cos(m\phi_i) + \overline{B}_{imn}\sin(m\phi_i)] - mr_i^{n-1}P_n^m(\mu_i)(1-\mu_i^2)^{-1/2}[\overline{C}_{imn}\sin(m\phi_i) - \overline{D}_{imn}\cos(m\phi_i)] + \frac{m(n+3)}{2\eta_i(n+1)(2n+3)}r_i^{n+1}P_n^m(\mu_i)(1-\mu_i^2)^{-1/2}[\overline{E}_{imn}\sin(m\phi_i) - \overline{F}_{imn}\cos(m\phi_i)]\Big\} \tag{11c}$$

$$\begin{bmatrix} v_r \\ v_\theta \\ v_\phi \end{bmatrix} = \sum_{j=1}^{N}\sum_{n=1}^{\infty}\sum_{m=0}^{n}\left\{A_{jmn}\begin{bmatrix} A_{jimn}^{(1)} \\ A_{jimn}^{(2)} \\ A_{jimn}^{(3)} \end{bmatrix} + B_{jmn}\begin{bmatrix} B_{jimn}^{(1)} \\ B_{jimn}^{(2)} \\ B_{jimn}^{(3)} \end{bmatrix} + \ldots + F_{jmn}\begin{bmatrix} F_{jimn}^{(1)} \\ F_{jimn}^{(2)} \\ F_{jimn}^{(3)} \end{bmatrix}\right\} \tag{12}$$

and $i = 1, 2, \ldots,$ or N. The functions $A_{jimn}^{(l)}(r_i,\theta_i,\phi_i)$, $B_{jimn}^{(l)}(r_i,\theta_i,\phi_i)$, $\ldots$, and $F_{jimn}^{(l)}(r_i,\theta_i,\phi_i)$ with $l = 1, 2,$ and 3 in Eq. 12 are defined by Eqs. C1 to C6 in Appendix C (Hassonjee et al., 1988; Keh and Yang, 1991).

To satisfy the boundary conditions of Eqs. 3a to 3c exactly along the entire interface of each droplet would require the solution of the entire infinite arrays of unknown coefficients A_{jmn}, B_{jmn}, $\ldots$, F_{jmn}, $\overline{A}_{imn}$, $\overline{B}_{imn}$, $\ldots$, and $\overline{F}_{imn}$. However, the multipole collocation method allows one to truncate the infinite series in Eqs. 11 and 12 into finite ones and then to enforce the boundary conditions at a finite number of discrete points on the surface of each sphere (O'Brien, 1968; Hassonjee et al., 1988). First, the order of summation $\Sigma_{n=1}^{\infty}\Sigma_{m=0}^{n}$ in Eqs. 11 and 12 is changed to $\Sigma_{m=0}^{\infty}\Sigma_{n=m,n\neq 0}^{\infty}$ without the loss of any terms in the series. Then, the infinite series $\Sigma_{m=0}^{\infty}$ is truncated after the M terms and the infinite series $\Sigma_{n=m,n\neq 0}^{\infty}$ is truncated after the K terms for each value of i or j. Application of Eqs. 3a, 3b and 3c to Eqs. 10 after this arrangement yields

$$\sum_{j=1}^{N}\sum_{m=0}^{M-1}\sum_{\substack{n=m\\n\neq 0}}^{m+K-1}[A_{jmn}A_{jimn}^{(1)} + B_{jmn}B_{jimn}^{(1)} + \ldots + F_{jmn}F_{jimn}^{(1)}]_{r_i=a_i} = \sum_{m=0}^{M-1}\sum_{\substack{n=m\\n\neq 0}}^{m+K-1}\Big\{na_i^{n-1}P_n^m(\mu_i)[\overline{C}_{imn}\cos(m\phi_i) + \overline{D}_{imn}\sin(m\phi_i)] + \frac{n}{2\eta_i(2n+3)}a_i^{n+1}P_n^m(\mu_i)[\overline{E}_{imn}\cos(m\phi_i) + \overline{F}_{imn}\sin(m\phi_i)]\Big\} \tag{13a}$$

$$\sum_{j=1}^{N}\sum_{m=0}^{M-1}\sum_{\substack{n=m\\n\neq 0}}^{m+K-1}[A_{jmn}A_{jimn}^{(2)} + B_{jmn}B_{jimn}^{(2)} + \ldots + F_{jmn}F_{jimn}^{(2)}]_{r_i=a_i} = \sum_{m=0}^{M-1}\sum_{\substack{n=m\\n\neq 0}}^{m+K-1}\Big\{-ma_i^nP_n^m(\mu_i)(1-\mu_i^2)^{-1/2}[\overline{A}_{imn}\sin(m\phi_i)$$

$$-\overline{B}_{imn}\cos(m\phi_i)] - a_i^{n-1}(1-\mu_i^2)^{1/2}\frac{dP_n^m(\mu_i)}{d\mu_i}[\overline{C}_{imn}\cos(m\phi_i)$$

$$+\overline{D}_{imn}\sin(m\phi_i)] - \frac{(n+3)}{2\eta_i(n+1)(2n+3)}a_i^{n+1}(1-\mu_i^2)^{1/2}\frac{dP_n^m(\mu_i)}{d\mu_i}$$

$$\times[\overline{E}_{imn}\cos(m\phi_i)+\overline{F}_{imn}\sin(m\phi_i)]\Bigg\} \quad (13b)$$

$$\sum_{j=1}^{N}\sum_{m=0}^{M-1}\sum_{\substack{n=m\\n\neq 0}}^{m+K-1}[A_{jmn}A_{jimn}^{(3)}+B_{jmn}B_{jimn}^{(3)}+\ldots+F_{jmn}F_{jimn}^{(3)}]_{r_i=a_i}$$

$$=\sum_{m=0}^{M-1}\sum_{\substack{n=m\\n\neq 0}}^{m+K-1}\Bigg\{a_i^n(1-\mu_i^2)^{1/2}\frac{dP_n^m(\mu_i)}{d\mu_i}[\overline{A}_{imn}\cos(m\phi_i)$$

$$+\overline{B}_{imn}\sin(m\phi_i)] - ma_i^{n-1}P_n^m(\mu_i)(1-\mu_i^2)^{-1/2}[\overline{C}_{imn}\sin(m\phi_i)$$

$$-\overline{D}_{imn}\cos(m\phi_i)] - \frac{m(n+3)}{2\eta_i(n+1)(2n+3)}a_i^{n+1}P_n^m(\mu_i)(1-\mu_i^2)^{-1/2}$$

$$\times[\overline{E}_{imn}\sin(m\phi_i)-\overline{F}_{imn}\cos(m\phi_i)]\Bigg\} \quad (13c)$$

$$\sum_{j=1}^{N}\sum_{m=0}^{M-1}\sum_{\substack{n=m\\n\neq 0}}^{m+K-1}[A_{jmn}A_{jimn}^{(1)}+B_{jmn}B_{jimn}^{(1)}+\ldots+F_{jmn}F_{jimn}^{(1)}]_{r_i=a_i}$$

$$=U_{ix}(1-\mu_i^2)^{1/2}\cos\phi_i+U_{iy}(1-\mu_i^2)^{1/2}\sin\phi_i+U_{iz}\mu_i \quad (13d)$$

$$\sum_{j=1}^{N}\sum_{m=0}^{M-1}\sum_{\substack{n=m\\n\neq 0}}^{m+K-1}\Bigg\{\left(\frac{\partial}{\partial r_i}-\frac{1}{r_i}\right)$$

$$\times[A_{jmn}A_{jimn}^{(2)}+B_{jmn}B_{jimn}^{(2)}+\ldots+F_{jmn}F_{jimn}^{(2)}]$$

$$-\frac{(1-\mu_i^2)^{1/2}}{r_i}\frac{\partial}{\partial\mu_i}[A_{jmn}A_{jimn}^{(1)}+B_{jmn}B_{jimn}^{(1)}+\ldots+F_{jmn}F_{jimn}^{(1)}]\Bigg\}_{r_i=a_i}$$

$$=\eta_i^*\sum_{m=0}^{M-1}\sum_{\substack{n=m\\n\neq 0}}^{m+K-1}\Bigg\{-m(n-1)a_i^{n-1}P_n^m(\mu_i)(1-\mu_i^2)^{-1/2}$$

$$\times[\overline{A}_{imn}\sin(m\phi_i)-\overline{B}_{imn}\cos(m\phi_i)] - 2(n-1)a_i^{n-2}(1-\mu_i^2)^{1/2}$$

$$\times\frac{dP_n^m(\mu_i)}{d\mu_i}[\overline{C}_{imn}\cos(m\phi_i)+\overline{D}_{imn}\sin(m\phi_i)] - \frac{n(n+2)}{\eta_i(n+1)(2n+3)}$$

$$\times a_i^n(1-\mu_i^2)^{1/2}\frac{dP_n^m(\mu_i)}{d\mu_i}[\overline{E}_{imn}\cos(m\phi_i)+\overline{F}_{imn}\sin(m\phi_i)]\Bigg\} \quad (13e)$$

$$\sum_{j=1}^{N}\sum_{m=0}^{M-1}\sum_{\substack{n=m\\n\neq 0}}^{m+K-1}\Bigg\{\left(\frac{\partial}{\partial r_i}-\frac{1}{r_i}\right)$$

$$\times[A_{jmn}A_{jimn}^{(3)}+B_{jmn}B_{jimn}^{(3)}+\ldots+F_{jmn}F_{jimn}^{(3)}]$$

$$+\frac{(1-\mu_i^2)^{-1/2}}{r_i}\frac{\partial}{\partial\phi_i}[A_{jmn}A_{jimn}^{(1)}+B_{jmn}B_{jimn}^{(1)}+\ldots+F_{jmn}F_{jimn}^{(1)}]\Bigg\}_{r_i=a_i}$$

$$=\eta_i^*\sum_{m=0}^{M-1}\sum_{\substack{n=m\\n\neq 0}}^{m+K-1}\Bigg\{(n-1)a_i^{n-1}(1-\mu_i^2)^{1/2}$$

$$\times\frac{dP_n^m(\mu_i)}{d\mu_i}[\overline{A}_{imn}\cos(m\phi_i)+\overline{B}_{imn}\sin(m\phi_i)]$$

$$-2m(n-1)a_i^{n-2}P_n^m(\mu_i)(1-\mu_i^2)^{-1/2}[\overline{C}_{imn}\sin(m\phi_i)$$

$$+\overline{D}_{imn}\cos(m\phi_i)] - \frac{mn(n+2)}{\eta_i(n+1)(2n+3)}a_i^n(1-\mu_i^2)^{-1/2}P_n^m(\mu_i)$$

$$\times[\overline{E}_{imn}\sin(m\phi_i)-\overline{F}_{imn}\cos(m\phi_i)]\Bigg\} \quad (13f)$$

where $\eta_i^*=\eta_i/\eta$ and $i=1, 2, \ldots,$ or N. This leaves a total of $6NK(2M-1)$ unknown constants $A_{jmn}, B_{jmn}, \ldots, F_{jmn}$ and $\overline{A}_{imn}, \overline{B}_{imn}, \ldots, \overline{F}_{imn}$ to be determined ($B_{j0n}=D_{j0n}=F_{j0n}=\overline{B}_{i0n}=\overline{D}_{i0n}=\overline{F}_{i0n}=0$).

Multiplying Eqs. 13 by the function sets $\cos(m'\phi_i)$ ($m'=0, 1, 2, \ldots, M-1$) and $\sin(m'\phi_i)$ ($m'=1, 2, \ldots, M-1$), integrating individually with respect to ϕ_i from 0 to 2π, and utilizing the orthogonality properties of these functions in this interval allow one to obtain $6(2M-1)$ equations. These equations can be satisfied at K discrete values of θ_i (rings) along the interface of each of the N droplets to result in a set of $6NK(2M-1)$ linear algebraic equations, which can be solved by any standard matrix-reduction method to obtain the equal-number unknown constants in terms of the droplet migration velocities $\underline{U}_i$. Once these constants are determined, the fluid velocity field is completely solved.

The accuracy of this boundary-collocation, truncated-series solution technique can be improved to any degree by choosing sufficiently large values of M and K. Naturally, the truncation error reduces to zero as $M\to\infty$ and $K\to\infty$. In general cases, the series in Eqs. 11 and 12 converge quite rapidly, and very good accuracy can be achieved with only a small number of terms in the Fourier series (M) and collocation rings on each droplet (K). Note that the value of K and the locations of the collocation rings can be varied for different spheres to improve the convergence of the expansion solution for some particular configurations of spheres.

One special case of the general three-dimensional theory described above is the case with planar symmetry, that is, the centers of all the fluid spheres lie in the plane $y=0$. For these planar symmetric configurations, $U_{iy}=0$, the coefficients A_{jmn}, D_{jmn}, F_{jmn}, $\overline{A}_{imn}$, $\overline{D}_{imn}$ and $\overline{F}_{imn}$ are all zero and the integration of Eqs. 13 after multiplication by $\sin(m'\phi_i)$ with respect to ϕ_i from 0 to 2π is trivial. Thus, the number of unknown coefficients (B_{jmn}, C_{jmn}, E_{jmn}, $\overline{B}_{imn}$, $\overline{C}_{imn}$ and $\overline{E}_{imn}$) is reduced to $6NKM$ and they are determined by an equal number of collocation equations. Furthermore, there are two special cases which can be deduced from the planar case: a string of fluid spheres translating parallel to their line of centers and a string of spheres moving normal to the line of centers. The fluid velocity distribution for the former case is axisymmetric and can be solved by employing the Stokes stream function, as formulated in Appendix A. For the case of a finite chain of droplets (the centers of all spheres lie on the z-axis) moving perpendicular to their line of centers ($\underline{U}_i=U_{ix}\underline{e}_x$), one has $\phi_i=\phi$, $b_i=c_i=b_{ij}=c_{ij}=0$ ($i, j=1, 2, \ldots, N$), and Eqs. 13 can be simplified to

$$\sum_{j=1}^{N}\sum_{n=1}^{K}[B_{j1n}B'_{jin}(a_i,\mu_i)+C_{j1n}C'_{jin}(a_i,\mu_i)+E_{j1n}E'_{jin}(a_i,\mu_i)]$$

$$=\sum_{n=1}^{K}\left[\overline{C}_{i1n}na_i^{n-1}P_n^1(\mu_i)+\overline{E}_{i1n}\frac{n}{2\eta_i(2n+3)}a_i^{n+1}P_n^1(\mu_i)\right] \quad (14a)$$

$$\sum_{j=1}^{N}\sum_{n=1}^{K}[B_{j1n}B''_{jin}(a_i,\mu_i)+C_{j1n}C''_{jin}(a_i,\mu_i)+E_{j1n}E''_{jin}(a_i,\mu_i)]$$

$$=\sum_{n=1}^{K}\left[\overline{B}_{i1n}a_i^nP_n^1(\mu_i)(1-\mu_i^2)^{-1/2}-\overline{C}_{i1n}a_i^{n-1}(1-\mu_i^2)^{1/2}\frac{dP_n^1(\mu_i)}{d\mu_i}\right.$$

$$\left.-\overline{E}_{i1n}\frac{(n+3)}{2\eta_i(n+1)(2n+3)}a_i^{n+1}(1-\mu_i^2)^{1/2}\frac{dP_n^1(\mu_i)}{d\mu_i}\right] \quad (14b)$$

$$\sum_{j=1}^{N}\sum_{n=1}^{K}[B_{j1n}B'''_{jin}(a_i,\mu_i)+C_{j1n}C'''_{jin}(a_i,\mu_i)+E_{j1n}E'''_{jin}(a_i,\mu_i)]$$

$$=\sum_{n=1}^{K}\left[\overline{B}_{i1n}a_i^n(1-\mu_i^2)^{1/2}\frac{dP_n^1(\mu_i)}{d\mu_i}-\overline{C}_{i1n}a_i^{n-1}P_n^1(\mu_i)(1-\mu_i^2)^{-1/2}\right.$$

$$\left.-\overline{E}_{i1n}\frac{(n+3)}{2\eta_i(n+1)(2n+3)}a_i^{n+1}P_n^1(\mu_i)(1-\mu_i^2)^{-1/2}\right] \quad (14c)$$

$$\sum_{j=1}^{N}\sum_{n=1}^{K}[B_{j1n}B'_{jin}(a_i,\mu_i)+C_{j1n}C'_{jin}(a_i,\mu_i)$$

$$+E_{j1n}E'_{jin}(a_i,\mu_i)]=U_{ix}(1-\mu_i^2)^{1/2} \quad (14d)$$

$$\sum_{j=1}^{N}\sum_{n=1}^{K}[B_{j1n}B^{*}_{jin}(a_i,\mu_i)+C_{j1n}C^{*}_{jin}(a_i,\mu_i)+E_{j1n}E^{*}_{jin}(a_i,\mu_i)]$$

$$=\eta_i^*\sum_{n=1}^{K}[\overline{B}_{i1n}(n-1)a_i^{n-1}P_n^1(\mu_i)(1-\mu_i^2)^{-1/2}$$

$$-\overline{C}_{i1n}2(n-1)a_i^{n-2}(1-\mu_i^2)^{1/2}\frac{dP_n^1(\mu_i)}{d\mu_i}$$

$$\left.-\overline{E}_{i1n}\frac{n(n+2)}{\eta_i(n+1)(2n+3)}a_i^n(1-\mu_i^2)^{1/2}\frac{dP_n^1(\mu_i)}{d\mu_i}\right] \quad (14e)$$

$$\sum_{j=1}^{N}\sum_{n=1}^{K}[B_{j1n}B^{**}_{jin}(a_i,\mu_i)+C_{j1n}C^{**}_{jin}(a_i,\mu_i)+E_{j1n}E^{**}_{jin}(a_i,\mu_i)]$$

$$=\eta_i^*\sum_{n=1}^{K}\left[\overline{B}_{i1n}(n-1)a_i^{n-1}(1-\mu_i^2)^{1/2}\frac{dP_n^1(\mu_i)}{d\mu_i}\right.$$

$$-\overline{C}_{i1n}2(n-1)a_i^{n-2}P_n^1(\mu_i)(1-\mu_i^2)^{-1/2}$$

$$\left.-\overline{E}_{i1n}\frac{n(n+2)}{\eta_i(n+1)(2n+3)}a_i^nP_n^1(\mu_i)(1-\mu_i^2)^{-1/2}\right] \quad (14f)$$

where the definitions of functions $B'_{jin}(r_i,\mu_i)$, $C'_{jin}(r_i,\mu_i)$, $E'_{jin}(r_i,\mu_i)$, $\ldots$, $E'''_{jin}(r_i,\mu_i)$ and $B^*_{jin}(r_i,\mu_i)$, $C^*_{jin}(r_i,\mu_i)$, $\ldots$, $E^{**}_{jin}(r_i,\mu_i)$ are given by Eqs. C7 to C21 and the dependence on ϕ factors out. Instead of using Eqs. 13, one can apply Eqs. 14 at K discrete values of θ_i (rings) along the interface of each droplet i for this special case. This generates a set of $6NK$ linear algebraic equations which can be solved for the $6NK$ unknown constants B_{j1n}, C_{j1n}, E_{j1n}, $\overline{B}_{i1n}$, $\overline{C}_{i1n}$, and $\overline{E}_{i1n}$.

The resistance problem

The resistance problems are defined as those in which the forces acting on the particles are to be determined for a specified particles' motion in the surrounding fluid. The general expression for the drag force exerted by the external fluid on the ith sphere is (Happel and Brenner, 1983)

$$\underline{F}_i=-4\pi\nabla[r_i^3p_{-2}^{(i)}],\ i=1,2,\ldots,N \quad (15)$$

That is, only a lowest-order external solid spherical harmonic function contributes to the force on each particle. Substituting Eq. 6a into Eq. 15 gives

$$\underline{F}_i=-4\pi(E_{i11}\underline{e}_x+F_{i11}\underline{e}_y+E_{i01}\underline{e}_z),\quad i=1,2,\ldots,N \quad (16)$$

in which the three coefficients for each of the N droplets are known for given droplet velocities from the solution of Eqs. 13. Note that the truncation procedure, employed in the previous subsection, does not affect the drag result if the obtained values of E_{i01}, E_{i11}, and F_{i11} are unchanged from their exact values.

The drag result can be expressed as

$$\underline{F}_i=\sum_{j=1}^{N}\underline{\underline{K}}_{ij}\cdot\underline{F}_j^{(0)},\quad i=1,2,\ldots,N \quad (17)$$

with

$$\underline{F}_j^{(0)}=-\frac{1}{m_j}\underline{U}_j \quad (18)$$

which is the drag force on droplet j in the absence of all the other ones. Obviously, from Eq. 1,

$$m_j=\frac{1}{6\pi\eta a_j}\frac{3\eta_j^*+3}{3\eta_j^*+2}. \quad (19)$$

The dimensionless resistance tensor $\underline{\underline{K}}_{ij}$ is a function of the relative viscosities, orientations, sizes and separation distances of the droplets. When the ith sphere is separated by an infinite distance from all of the others, one has

$$\underline{\underline{K}}_{ii}=\underline{\underline{I}} \quad (20a)$$

and

$$\underline{\underline{K}}_{ij}=\underline{\underline{0}} \quad (20b)$$

for $i, j=1, 2, \ldots, N$ and $j\neq i$.

The mobility problem

The mobility problem is defined as that in which the forces acting on the particles are prescribed and the particles' motion in the ambient fluid is to be determined. The presentation of the mobility problem is rather awkward since the boundary conditions involve the unknowns, but in many physical problems the forces are the prescribed quantities and the particles must move accordingly. In a mobility problem, Eq. 16 still gives the drag force exerted by the external fluid on the ith sphere, which is equal in magnitude but opposite in direction to the applied force on the particle in the quasisteady limit. However, the coefficients E_{i01}, E_{i11} and F_{i11} obtained from Eqs.

13 contain the unknown translational velocities of the N droplets (3N components in total). These unknown velocities can be determined by solving the 3N scalar equations resulting from Eq. 16 simultaneously for a given set of $\underline{F}_j$.

The result of the particles' motion can be written as

$$\underline{U}_i = \sum_{j=1}^{N} \underline{\underline{M}}_{ij} \cdot \underline{U}_j^{(0)}, \quad i = 1, 2, \ldots, N \tag{21}$$

with

$$\underline{U}_j^{(0)} = -m_j \underline{F}_j \tag{22}$$

which is the translational velocity of the jth droplet subject to an applied force $-\underline{F}_j$ in the absence of the other droplets. Similar to the resistance tensor $\underline{\underline{K}}_{ij}$, the dimensionless mobility tensor $\underline{\underline{M}}_{ij}$ is a function of the relative viscosities, orientations, sizes and separation distances of the droplets as well. Also, when the droplet i is separated by an infinite distance from all of the other droplets,

$$\underline{\underline{M}}_{ii} = \underline{\underline{I}} \tag{23a}$$

and

$$\underline{\underline{M}}_{ij} = \underline{\underline{0}} \tag{23b}$$

for $i, j = 1, 2, \ldots, N$ and $j \neq i$.

Results for Two Droplets

In this section we consider the slow motion of two fluid spheres which are oriented arbitrarily relative to the directions of their movement. For this simple case, the dimensionless resistance and mobility tensors defined by Eqs. 17 and 21 can be expressed as

$$\underline{\underline{K}}_{ij} = K_{ij}^{(p)} \underline{e}\underline{e} + K_{ij}^{(n)} (\underline{\underline{I}} - \underline{e}\underline{e}) \tag{24}$$

$$\underline{\underline{M}}_{ij} = M_{ij}^{(p)} \underline{e}\underline{e} + M_{ij}^{(n)} (\underline{\underline{I}} - \underline{e}\underline{e}) \tag{25}$$

where i and j equal 1 or 2 and $\underline{e}$ is the unit vector directed from the center of sphere 1 toward the center of sphere 2. Because axisymmetric motions are not coupled to transverse ones, as illustrated by the above equations, it is easy to show from using Eqs. 17, 18, 21 and 22, that the following scalar relations between the dimensionless resistance and mobility tensors always hold for two arbitrary fluid spheres:

$$K_{11}^{(p,n)} = [M_{11}^{(p,n)} - M_{12}^{(p,n)} M_{21}^{(p,n)} / M_{22}^{(p,n)}]^{-1} \tag{26a}$$

$$K_{12}^{(p,n)} = \frac{m_2}{m_1} [M_{21}^{(p,n)} - M_{11}^{(p,n)} M_{22}^{(p,n)} / M_{12}^{(p,n)}]^{-1} \tag{26b}$$

or

$$M_{11}^{(p,n)} = [K_{11}^{(p,n)} - K_{12}^{(p,n)} K_{21}^{(p,n)} / K_{22}^{(p,n)}]^{-1} \tag{27a}$$

$$M_{12}^{(p,n)} = \frac{m_1}{m_2} [K_{21}^{(p,n)} - K_{11}^{(p,n)} K_{22}^{(p,n)} / K_{12}^{(p,n)}]^{-1}. \tag{27b}$$

The corresponding expressions for $K_{22}^{(p,n)}$, $K_{21}^{(p,n)}$, $M_{22}^{(p,n)}$, and $M_{21}^{(p,n)}$ can be obtained from the above formulae by interchanging the subscripts 1 and 2. Thus, one can solve either the resistance or the mobility problem first and then use the relations 26 or 27 to obtain the solution for the other.

Using a method of reflections, the explicit formulae for the two-droplet resistance parameters $K_{11}^{(p)}$, $K_{12}^{(p)}$, $K_{11}^{(n)}$, and $K_{12}^{(n)}$ were derived in power series of r_{12} up to $O(r_{12}^{-5})$, where r_{12} is the center-to-center distance between the two fluid spheres (Hetsroni and Haber, 1978). The corresponding formulae of mobility parameters $M_{11}^{(p)}$, $M_{12}^{(p)}$, $M_{11}^{(n)}$, and $M_{12}^{(n)}$ for two identical droplets were also obtained in power series of r_{12} up to $O(r_{12}^{-7})$ by employing the connector algebra (Geigenmuller and Mazur, 1986). On the other hand, the exact solution of the resistance parameters $K_{11}^{(p)}$, $K_{12}^{(p)}$, $K_{21}^{(p)}$, and $K_{22}^{(p)}$ was obtained by solving the axisymmetric creeping motion of two droplets using spherical bipolar coordinates (Haber et al., 1973). Here, the numerical results of the mobility parameters $M_{11}^{(p,n)}$, $M_{12}^{(p,n)}$, $M_{21}^{(p,n)}$, and $M_{22}^{(p,n)}$ will be presented using the collocation method described in the previous section. The solutions given by Haber et al. (1973) and Geigenmuller and Mazur (1986) can provide a convenient means of testing the accuracy of the present numerical solution technique.

For the axisymmetric motion of two fluid spheres, the flow field of the fluid phases is given by the truncated form of Eqs. A6 with coefficients β_{jn}, δ_{in}, α_{in} and γ_{in} determined by Eqs. A9. Once these coefficients are determined in terms of the droplet migration velocities $\underline{U}_i$ $(= U_{iz}\underline{e}_z)$, solution of Eqs. A12 will result in these droplet velocities for a given set of forces $\underline{F}_i$. Likewise, to evaluate the migration velocities for the motion of two fluid spheres perpendicular to their line of centers, Eqs. 14 can be used to determine the coefficients B_{j1n}, C_{j1n}, E_{j1n}, $\overline{B}_{i1n}$, $\overline{C}_{i1n}$ and $\overline{E}_{i1n}$ for the fluid velocity field and solution of Eqs. 16 will yield the droplet velocities $\underline{U}_i$ $(= U_{ix}\underline{e}_x)$. When specifying the discrete values of θ_i (rings) on the surface of each droplet i where conditions 3a to 3c are to be exactly satisfied, a pattern which is symmetric about the equatorial plane $\theta_i = \pi/2$ should be chosen to preserve the geometric symmetry of the spherical boundary shape. A detailed examination of the system of the linear algebraic Eqs. 14 or A9 shows that locating rings at $\theta_i = 0$, $\pi/2$ or π can produce a singular coefficient matrix. In order to avoid this obstacle, rings at $\theta_i = \alpha$, $\pi/2 - \alpha$, $\pi/2 + \alpha$ and $\pi - \alpha$ are taken to be the four basic multipoles. Additional rings along each droplet interface are selected as mirror-image pairs about the plane $\theta_i = \pi/2$ to divide the two semispheres into shells with equal arcs. The optimum values of α in this work are found to be $0.01° \sim 0.1°$, with which the numerical results of all mobility parameters converge satisfactorily.

A number of numerical solutions for the interaction parameters $M_{11}^{(p)}$, $M_{12}^{(p)}$, $M_{11}^{(n)}$ and $M_{12}^{(n)}$ are presented in Table 1 for the translation of two identical droplets ($a_1 = a_2 = a$, $\eta_1^* = \eta_2^* = \eta^*$) at various relative viscosities and spacings using the collocation technique. For this symmetric case, one has $M_{11}^{(p,n)} = M_{22}^{(p,n)}$ and $M_{12}^{(p,n)} = M_{21}^{(p,n)}$. The Crout method (Gerald and Wheatley, 1989) has been employed to solve the matrix equations and a DEC 5000/200 workstation was utilized to perform the calculations. The accuracy and convergence behavior of the truncation depends principally upon the relative spacing of the spheres. All of the results of the mobility parameters obtained under this numerical scheme converge to at least five digits after the

Table 1. The Droplet Mobility Parameters for the Slow Motion of Two Identical Fluid Spheres ($a_1=a_2=a$, $\eta_1^*=\eta_2^*=\eta^*$) as Computed from Using the Multipole Collocation Technique*

		Collocation Technique				Bipolar Coordinates		Connector Algebra	
η^*	$2a/r_{12}$	$M_{11}^{(p)}$	$M_{12}^{(p)}$	$M_{11}^{(n)}$	$M_{12}^{(n)}$	$M_{11}^{(p)}$	$M_{12}^{(p)}$	$M_{11}^{(n)}$	$M_{12}^{(n)}$
0.5	0.2	0.99983	0.11633	1.00000	0.05850	0.99983	0.11633	1.00000	0.05850
	0.4	0.99721	0.23074	1.00000	0.11800	0.99721	0.23074	1.00000	0.11800
	0.6	0.98593	0.34231	1.00000	0.17950	0.98593	0.34231	0.99998	0.17950
	0.8	0.95408	0.45670	1.00005	0.24399	0.95408	0.45670	0.99990	0.24400
	0.9	0.91967	0.52543	1.00020	0.27766	0.91967	0.52543	0.99979	0.27769
	0.95	0.88812	0.57256	1.00033	0.29489	0.88812	0.57256	0.99971	0.29495
	0.99	0.82986	0.64258	1.00044	0.30883	0.82987	0.64259	0.99963	0.30896
	1.0	0.73765	0.73765	1.00051	0.31238	—	—	0.99950	0.31316
1.0	0.2	0.99978	0.12450	1.00000	0.06275	0.99978	0.12450	1.00000	0.06275
	0.4	0.99658	0.24610	0.99999	0.12700	0.99658	0.24610	0.99999	0.12700
	0.6	0.98315	0.36330	0.99990	0.19425	0.98315	0.36330	0.99990	0.19425
	0.8	0.94683	0.48258	0.99940	0.26598	0.94683	0.48258	0.99942	0.26600
	0.9	0.90894	0.55446	0.99865	0.30395	0.90894	0.55446	0.99883	0.30403
	0.95	0.87517	0.60362	0.99792	0.32347	0.87517	0.60362	0.99838	0.32367
	0.99	0.81681	0.67357	0.99693	0.33920	0.81681	0.67357	0.99793	0.33970
	1.0	0.74659	0.74659	0.99655	0.34308	—	—	0.99780	0.34375
5.0	0.2	0.99969	0.14083	1.00000	0.07125	0.99969	0.14083	1.00000	0.07125
	0.4	0.99516	0.27685	0.99996	0.14500	0.99516	0.27685	0.99996	0.14500
	0.6	0.97708	0.40554	0.99953	0.22375	0.97708	0.40554	0.99959	0.22375
	0.8	0.93158	0.53552	0.99677	0.31010	0.93158	0.53552	0.99768	0.31000
	0.9	0.88713	0.61394	0.99209	0.35724	0.88713	0.61394	0.99530	0.35672
	0.95	0.85053	0.66587	0.98733	0.38228	0.85053	0.66587	0.99349	0.38111
	0.99	0.79883	0.72913	0.98040	0.40341	0.79882	0.72913	0.99167	0.40116
	1.0	0.76538	0.76538	0.97763	0.40900	—	—	0.98996	0.40753

*(This work) and the spherical bipolar coordinates (Haber et al., 1973) or the connector algebra (Geigenmuller and Mazur, 1986).

decimal point. For the case of two touching spheres (the most difficult case), the number of multipoles $K=150$ is sufficiently large to achieve this convergence. As expected, the results in Table 1 illustrate that the interaction of droplets increases, for all values of η^*, with decreasing gap thickness between them.

The exact solutions for $M_{11}^{(p)}$ and $M_{12}^{(p)}$ calculated from the results of the resistance parameters obtained by Haber et al. (1973) and the asymptotic solutions for $M_{11}^{(n)}$ and $M_{12}^{(n)}$ given by Geigenmuller and Mazur (1986) are also listed in Table 1 for comparison. It can be seen that the results from the collocation technique agree remarkably well with the exact solutions for all droplet viscosities and spacings. Also, the collocation results are in good agreement with the asymptotic solutions from the connector algebra for the case of large to

Table 2. The Particle Mobility Parameters for the Slow Motion of Two Spherical Gas Bubbles ($\eta_1^*=\eta_2^*\to 0$)

$\frac{a_2}{a_1}$	$\frac{a_1+a_2}{r_{12}}$	$M_{11}^{(p)}$	$M_{12}^{(p)}$	$M_{22}^{(p)}$	$M_{11}^{(n)}$	$M_{12}^{(n)}$	$M_{22}^{(n)}$
1.0	0.2	0.99990	0.10000	0.99990	1.00000	0.05000	1.00000
	0.4	0.99833	0.20003	0.99833	1.00001	0.10000	1.00001
	0.6	0.99106	0.30059	0.99106	1.00011	0.15000	1.00011
	0.8	0.96830	0.40599	0.96830	1.00068	0.20002	1.00068
	0.9	0.94218	0.46810	0.94218	1.00150	0.22511	1.00150
	0.95	0.91806	0.50886	0.91806	1.00219	0.23774	1.00219
	0.99	0.87444	0.56516	0.87444	1.00300	0.24799	1.00300
	1.0	0.72135	0.72135	0.72135	1.00327	0.25060	1.00327
2.0	0.2	0.99984	0.13333	0.99996	1.00000	0.06667	1.00000
	0.4	0.99728	0.26669	0.99936	1.00003	0.13333	1.00000
	0.6	0.98471	0.40057	0.99665	1.00034	0.20000	1.00002
	0.8	0.94172	0.53943	0.98875	1.00244	0.26669	1.00010
	0.9	0.88867	0.61905	0.98027	1.00589	0.30010	1.00021
	0.95	0.83828	0.66975	0.97266	1.00910	0.31691	1.00030
	0.99	0.74776	0.73731	0.95885	1.01304	0.33050	1.00041
	1.0	0.45536	0.91010	0.91010	1.01440	0.33396	1.00044
5.0	0.2	0.99984	0.11667	0.99999	1.00000	0.08333	1.00000
	0.4	0.99722	0.33334	0.99990	1 00004	0.16667	1.00000
	0.6	0.98332	0.50020	0.99949	1.00061	0.25000	1.00000
	0.8	0.92811	0.66915	0.99837	1.00547	0.33334	1.00000
	0.9	0.84903	0.75902	0.99727	1.01582	0.37503	1.00001
	0.95	0.76721	0.81087	0.99635	1.02769	0.39591	1.00001
	0.99	0.61570	0.87145	0.99466	1.04507	0.41272	1.00001
	1.0	0.19775	0.98875	0.98875	1.05199	0.41700	1.00002

Table 3. The Particle Mobility Parameters for the Slow Motion of Two Solid Spheres ($\eta_1^* = \eta_2^* \rightarrow \infty$)

$\frac{a_2}{a_1}$	$\frac{a_1+a_2}{r_{12}}$	$M_{11}^{(p)}$	$M_{12}^{(p)}$	$M_{22}^{(p)}$	$M_{11}^{(n)}$	$M_{12}^{(n)}$	$M_{22}^{(n)}$	Q_{11}	Q_{12}	Q_{22}
1.0	0.2	0.9996	0.1490	0.9996	1.0000	0.0755	1.0000	0.0000	0.0075	0.0000
	0.4	0.9944	0.2922	0.9944	0.9999	0.1540	0.9999	−0.0001	0.0299	0.0001
	0.6	0.9738	0.4268	0.9738	0.9991	0.2385	0.9991	−0.0007	0.0675	0.0007
	0.8	0.9234	0.5627	0.9234	0.9939	0.3325	0.9939	−0.0069	0.1203	0.0069
	0.9	0.8755	0.6447	0.8755	0.9848	0.3856	0.9848	−0.0200	0.1534	0.0200
	0.95	0.8378	0.6978	0.8378	0.9748	0.4161	0.9748	−0.0358	0.1729	0.0358
	0.99	0.7916	0.7557	0.7916	0.9549	0.4483	0.9549	−0.0697	0.1932	0.0697
	0.995	0.7837	0.7650	0.7837	0.9485	0.4549	0.9485	−0.0813	0.1971	0.0813
	1.0	0.7750	0.7750	0.7750	0.8907	0.4896	0.8907	−0.2002	0.2008	0.2002
2.0	0.2	0.9994	0.1985	0.9999	1.0000	0.1007	1.0000	0.0000	0.0067	0.0000
	0.4	0.9905	0.3884	0.9979	0.9998	0.2059	1.0000	−0.0000	0.0266	0.0001
	0.6	0.9518	0.5636	0.9914	0.9975	0.3200	0.9998	−0.0006	0.0600	0.0010
	0.8	0.8413	0.7305	0.9791	0.9833	0.4483	0.9979	−0.0070	0.1060	0.0083
	0.9	0.7256	0.8224	0.9701	0.9602	0.5222	0.9941	−0.0216	0.1322	0.0228
	0.95	0.6321	0.8778	0.9638	0.9358	0.5656	0.9894	−0.0398	0.1444	0.0405
	0.99	0.5174	0.9351	0.9563	0.8911	0.6147	0.9787	−0.0756	0.1488	0.0807
	0.995	0.4944	0.9455	0.9547	0.8775	0.6259	0.9748	−0.0863	0.1469	0.1240
	1.0	0.4768	0.9536	0.9536	0.8614*	0.6387*	0.9701*	−0.0990*	0.1442*	0.1801*
5.0	0.2	0.9994	0.2476	1.0000	1.0000	0.1262	1.0000	0.0000	0.0042	0.0000
	0.4	0.9902	0.4808	1.0000	0.9997	0.2596	1.0000	−0.0000	0.0167	0.0000
	0.6	0.9461	0.6861	0.9989	0.9956	0.4075	1.0000	−0.0003	0.0375	0.0006
	0.8	0.7983	0.8543	0.9981	0.9667	0.5780	0.9995	−0.0037	0.0663	0.0049
	0.9	0.6217	0.9252	0.9980	0.9132	0.6775	0.9987	−0.0136	0.0820	0.0124
	0.95	0.4688	0.9594	0.9980	0.8522	0.7362	0.9977	−0.0282	0.0877	0.0213
	0.99	0.2720	0.9891	0.9979	0.7342	0.8035	0.9951	−0.0565	0.0823	0.0425
	0.995	0.2153	0.9959	0.9979	0.6983	0.8189	0.9942	−0.0654	0.0790	0.0501
	1.0	0.1996	0.9979	0.9979	0.6557*	0.8365*	0.9931*	−0.0766*	0.0749*	0.0593*

*Values evaluated by extrapolation from results for $(a_1+a_2)/r_{12} = 0.9$ to 0.995.

moderate droplet separations. However, the accuracy of the asymptotic solutions begins to deteriorate, as expected, when the droplets are close together (especially for the case of $M_{11}^{(p)}$ and $M_{12}^{(p)}$ which is not shown in Table 1). Note that the problem of two touching spheres cannot be solved by utilizing spherical bipolar coordinates.

In Table 2 we list the numerical solutions of the interaction parameters $M_{11}^{(p,n)}$, $M_{12}^{(p,n)}$ and $M_{22}^{(p,n)}$ for the limiting case of two gas bubbles ($\eta_1^* = \eta_2^* \rightarrow 0$) at various relative radii and spacings. It can be predicted by the reciprocal theorem of Lorentz (Happel and Brenner, 1983) that $M_{21}^{(p,n)}/M_{12}^{(p,n)} = m_2/m_1$ for any two drops in Stokes flow. Note that $m_2/m_1 = a_1/a_2$ for two spheres of identical viscosities. The collocation results of the mobility parameters for the other limiting case of two torque-free rigid spheres ($\eta_1^* = \eta_2^* \rightarrow \infty$) are presented in Table 3. The formulation of the collocation procedure for the motion of multiple rigid spheres in an arbitrary configuration is given in Appendix B and the dimensionless rotational mobility tensors $\underline{\underline{Q}}_{ij}$, defined by Eq. B9b, for the case of two spheres can be expressed as

$$\underline{\underline{Q}}_{ij} = Q_{ij}(\underline{\underline{I}} - \underline{e}\underline{e}), \quad i, j = 1 \text{ or } 2. \tag{28}$$

From the reciprocal theorem of Lorentz, one has $Q_{21}/Q_{12} = -a_2/a_1$. The results in Table 3 agree very well with the analysis of Maude (1961), Goldman et al. (1966) and Davis (1969) for the motion of two solid spheres using bipolar coordinates. Note that the exact (numerical) solutions for the asymmetric motion of two arbitrary solid or fluid spheres in contact ($2a/r_{12} = 1$) have never been reported before.

The normalized velocities of two identical spheres moving with equal applied forces in the directions parallel and perpendicular to their line of centers as a function of the separation parameter $2a/d$ (in which $d = r_{12}$) are plotted by dashed curves in Figures 2 and 3, respectively. Three constant values, 0, 1 and ∞, are chosen for η^* in these curves. It can be seen that the migration velocity of each sphere is a monotonic increasing function of $2a/d$, as shown in Figure 2a or 2b, for the motion of two spheres along their line of centers. This trend can also be found for the motion of two fluid spheres perpendicular to their line of centers, as illustrated in Figure 3a or 3b. However, for the case of motion of two solid spheres normal to their line of centers, the translational velocity of each particle is a monotonic increasing function of $2a/d$ only for $2a/d \lesssim 0.993$; beyond this region, the particle mobility decreases with increasing $2a/d$. Also, as shown in Figure 3c, the angular velocity of each solid sphere is a monotonic increasing function of $2a/d$ for all $2a/d \lesssim 0.94$ and a monotonic decreasing function of $2a/d$ when the particles are closer to each other. When the two identical solid spheres are touching, they move as a rigid body (Goldman et al., 1966; Jeffrey and Onishi, 1984) with $U_1 = U_2 \simeq 1.38U^{(0)}$ and their angular velocities vanish.

The interaction effects between pairs of droplets can be extended to the evaluation of the mean settling velocity in a bounded dispersion of small droplets. In a later section, formulae for this mean velocity correct to the order of first power of the volume fraction of the droplets will be presented.

Results for Multiple Droplets

In the previous section solutions for the problem of slow motion of two spherical droplets based on the collocation

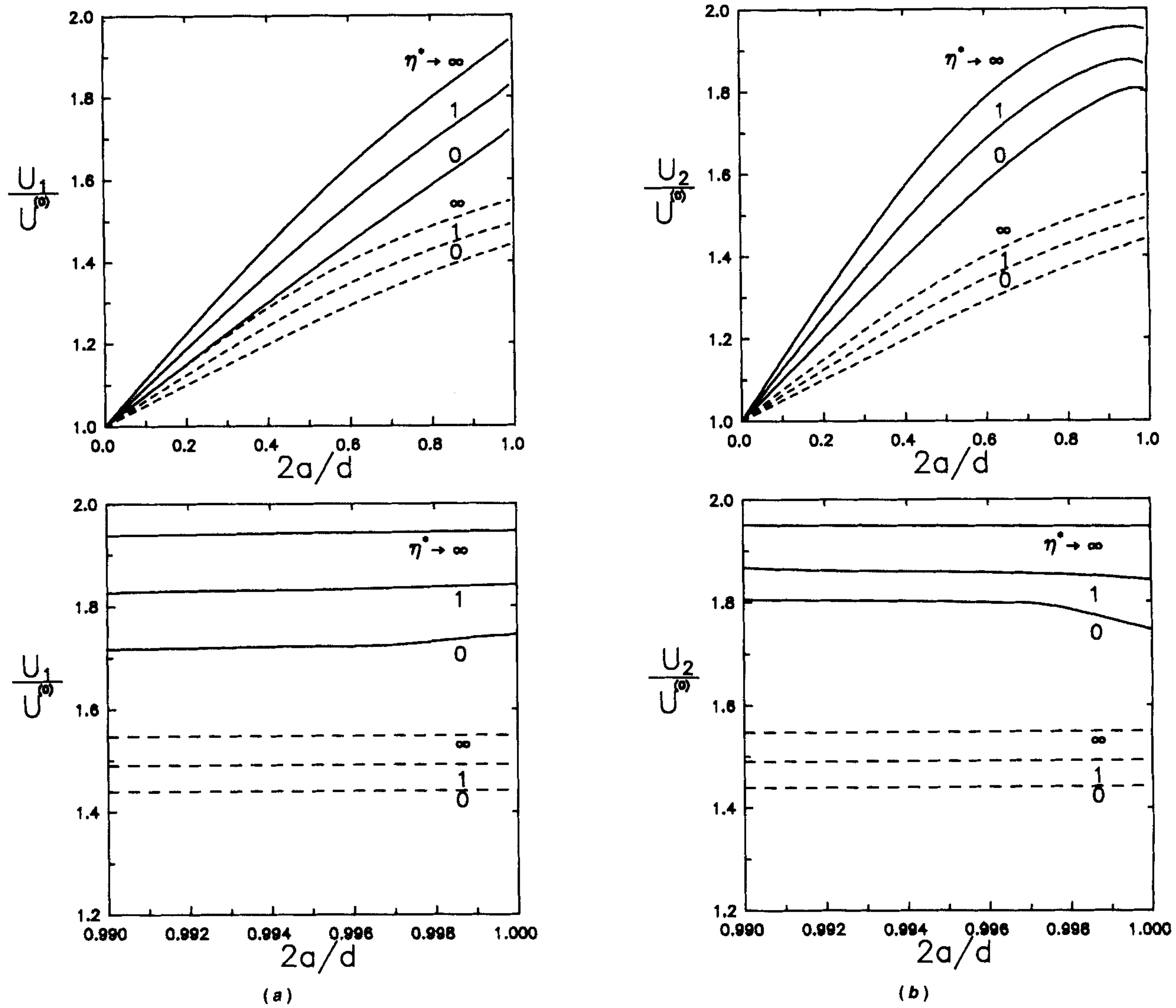

Figure 2. Normalized migration velocities of three identical coaxial spheres at equal spacings moving with equal applied forces along their line of centers vs. the separation parameter $2a/d$ with the relative viscosity η^* as a parameter: (a) sphere 1 (or sphere 3); (b) sphere 2.

The dashed curves are plotted for the migration velocities when only two spheres are present for comparison.

technique have been presented and were shown to be in perfect agreement with the available exact and asymptotic solutions. This section will examine the solutions for the migration of three or more droplets using the same collocation method. Since the number of droplet interaction parameters in the general problem is so great, here we only consider the motion of a linear chain of fluid spheres with equal spacings. Thus, Eqs. 24 and 25 (with $i, j = 1, 2, \ldots,$ or N) are still applicable for all the resistance and mobility tensors of the spheres. For the motion of an assemblage of three or more droplets, orientations other than a straight line may represent more stable configurations. The purpose of considering linear chains of multiple spheres is to demonstrate the application of collocation technique for systems containing three or more droplets rather than to infer that such chains represent stable configurations for the motion of multiple droplets.

From Eqs. 21 and 25, nine droplet mobility tensors, and therefore, eighteen mobility parameters, are needed in the general problem to express the motion of a chain of three spheres. For conciseness, we only consider the migration of three coaxial droplets of the same fluid in a symmetric configuration that the two end spheres are equal in radii ($a_1 = a_3$) and have the same distance from the central one ($r_{12} = r_{23}$). For this symmetric case, it is obvious that

$$M_{11}^{(p,n)} = M_{33}^{(p,n)} \tag{29a}$$

$$M_{12}^{(p,n)} = M_{32}^{(p,n)} \tag{29b}$$

$$M_{23}^{(p,n)} = M_{21}^{(p,n)} \tag{29c}$$

$$M_{31}^{(p,n)} = M_{13}^{(p,n)} \tag{29d}$$

In Tables 4 and 5, numerical results of the mobility parameters for the motions of three gas bubbles and three solid spheres,

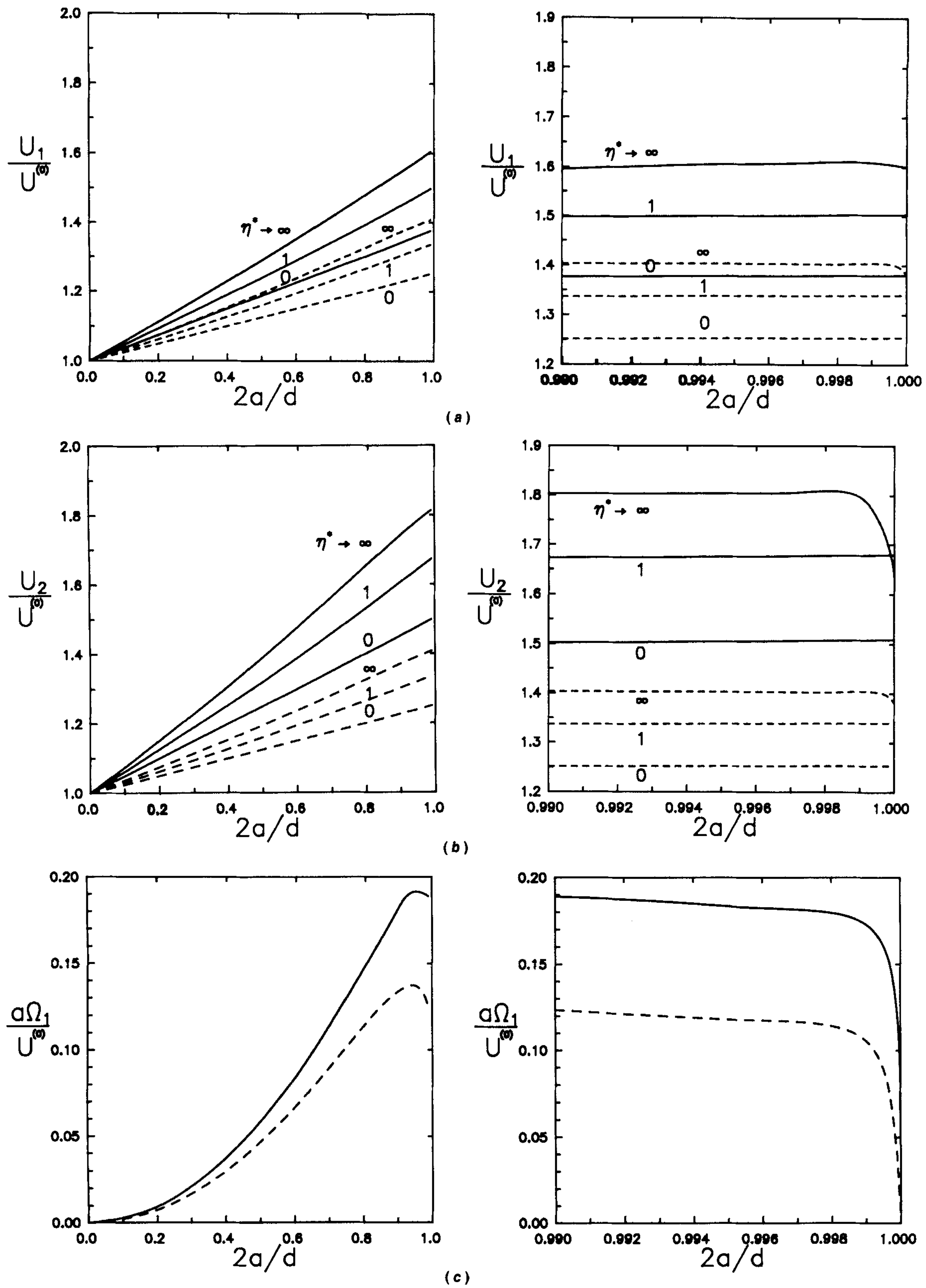

Figure 3. Normalized translational and rotational velocities of three identical coaxial spheres at equal spacings moving with equal applied forces normal to their line of centers vs. the separation parameter $2a/d$ with the relative viscosity η^* as a parameter: (a) translational velocity of sphere 1 (or sphere 3); (b) translational velocity of sphere 2; (c) rotational velocity of sphere 1 (or sphere 3) for the case of solid spheres ($\eta^* \rightarrow \infty$).

The dashed curves are plotted for the particle velocities when only two spheres are present for comparison.

Table 4. The Particle Mobility Parameters for the Slow Motion of Three Coaxial Bubbles ($\eta_1^* = \eta_2^* = \eta_3^* \to 0$) with $a_1 = a_3$ and $r_{12} = r_{23}$

$a_1{:}a_2{:}a_3$	$\frac{a_1+a_2}{r_{12}}$	$M_{11}^{(p)}$	$M_{22}^{(p)}$	$M_{12}^{(p)}$	$M_{21}^{(p)}$	$M_{13}^{(p)}$	$M_{11}^{(n)}$	$M_{22}^{(n)}$	$M_{12}^{(n)}$	$M_{21}^{(n)}$	$M_{13}^{(n)}$
1:1:1	0.2	1.000	1.000	0.100	0.100	0.050	1.000	1.000	0.050	0.050	0.025
	0.4	0.998	0.997	0.200	0.200	0.102	1.000	1.000	0.100	0.100	0.050
	0.6	0.990	0.982	0.298	0.298	0.158	1.000	1.000	0.150	0.150	0.075
	0.8	0.964	0.939	0.395	0.395	0.226	1.001	1.001	0.200	0.200	0.100
	0.9	0.933	0.891	0.447	0.447	0.273	1.002	1.003	0.225	0.225	0.113
	0.95	0.903	0.850	0.477	0.477	0.308	1.002	1.004	0.238	0.238	0.120
	0.99	0.844	0.781	0.512	0.512	0.362	1.003	1.006	0.248	0.248	0.125
	1.00	0.582	0.582	0.582	0.582	0.582	1.003	1.007	0.251	0.251	0.126
1:2:1	0.2	1.000	1.000	0.133	0.067	0.033	1.000	1.000	0.067	0.033	0.017
	0.4	0.997	0.999	0.267	0.133	0.069	1.000	1.000	0.133	0.067	0.033
	0.6	0.985	0.993	0.399	0.200	0.111	1.000	1.000	0.200	0.100	0.050
	0.8	0.941	0.978	0.534	0.267	0.168	1.002	1.000	0.267	0.133	0.068
	0.9	0.886	0.961	0.609	0.304	0.208	1.006	1.000	0.300	0.150	0.077
	0.95	0.833	0.947	0.654	0.327	0.237	1.009	1.001	0.317	0.159	0.082
	0.99	0.738	0.922	0.711	0.355	0.280	1.013	1.001	0.331	0.165	0.085
	1.00	0.419	0.838	0.838	0.419	0.419	1.015	1.001	0.335	0.167	0.087
2:1:2	0.2	1.000	1.000	0.067	0.133	0.067	1.000	1.000	0.033	0.067	0.033
	0.4	0.999	0.995	0.133	0.265	0.134	1.000	1.000	0.067	0.133	0.067
	0.6	0.995	0.970	0.197	0.393	0.203	1.000	1.001	0.100	0.200	0.100
	0.8	0.981	0.891	0.256	0.512	0.279	1.000	1.005	0.134	0.267	0.133
	0.9	0.964	0.801	0.284	0.567	0.326	1.000	1.012	0.151	0.301	0.150
	0.95	0.947	0.725	0.297	0.595	0.357	1.000	1.018	0.159	0.318	0.159
	0.99	0.911	0.607	0.311	0.621	0.403	1.001	1.026	0.166	0.333	0.165
	1.00	0.657	0.329	0.329	0.657	0.657	1.001	1.031	0.168	0.337	0.167

Table 5. The Particle Mobility Parameters for the Slow Motion of Three Coaxial Solid Spheres ($\eta_1^* = \eta_2^* = \eta_3^* \to \infty$) with $a_1 = a_3$ and $r_{12} = r_{23}$

$a_1{:}a_2{:}a_3$	$\frac{a_1+a_2}{r_{12}}$	$M_{11}^{(p)}$	$M_{22}^{(p)}$	$M_{12}^{(p)}$	$M_{21}^{(p)}$	$M_{13}^{(p)}$	$M_{11}^{(n)}$	$M_{22}^{(n)}$	$M_{12}^{(n)}$	$M_{21}^{(n)}$	$M_{13}^{(n)}$
1:1:1	0.2	1.000	0.999	0.149	0.149	0.075	1.000	1.000	0.076	0.076	0.038
	0.4	0.994	0.989	0.291	0.291	0.154	1.000	1.000	0.154	0.154	0.076
	0.6	0.970	0.949	0.418	0.418	0.244	0.999	0.998	0.239	0.239	0.114
	0.8	0.906	0.859	0.529	0.529	0.362	0.994	0.988	0.332	0.332	0.153
	0.9	0.835	0.784	0.584	0.584	0.452	0.984	0.969	0.385	0.385	0.175
	0.95	0.772	0.730	0.613	0.613	0.523	0.973	0.947	0.417	0.417	0.187
	0.99	0.684	0.669	0.641	0.641	0.614	0.951	0.899	0.452	0.452	0.192
	0.995	0.657	0.653	0.646	0.646	0.640	0.944	0.881	0.461	0.461	0.201
	1.00	0.649	0.649	0.649	0.649	0.649	0.872	0.544	0.541	0.541	0.216
1:2:1	0.2	0.999	1.000	0.198	0.099	0.051	1.000	1.000	0.101	0.050	0.025
	0.4	0.990	0.996	0.388	0.194	0.107	1.000	1.000	0.206	0.103	0.050
	0.6	0.951	0.983	0.559	0.280	0.179	0.997	1.000	0.320	0.160	0.074
	0.8	0.837	0.959	0.717	0.359	0.275	0.983	0.996	0.449	0.224	0.097
	0.9	0.716	0.942	0.800	0.400	0.342	0.960	0.988	0.524	0.262	0.107
	0.95	0.619	0.931	0.848	0.424	0.388	0.935	0.978	0.569	0.285	0.109
	0.99	0.477	0.916	0.900	0.450	0.454	0.888	0.952	0.625	0.313	0.114
	0.995	0.461	0.913	0.910	0.452	0.454	0.874	0.945	0.639	0.319	0.117
	1.00	0.456	0.912	0.912	0.456	0.456	0.857*	0.937*	0.655*	0.328*	0.121*
2:1:2	0.2	1.000	0.999	0.099	0.198	0.100	1.000	1.000	0.050	0.101	0.050
	0.4	0.997	0.981	0.192	0.384	0.200	1.000	1.000	0.103	0.206	0.101
	0.6	0.984	0.909	0.270	0.539	0.302	1.000	0.995	0.160	0.319	0.154
	0.8	0.950	0.730	0.326	0.651	0.415	0.997	0.967	0.222	0.444	0.211
	0.9	0.907	0.582	0.345	0.689	0.493	0.992	0.922	0.257	0.513	0.242
	0.95	0.860	0.485	0.352	0.704	0.557	0.986	0.876	0.276	0.551	0.261
	0.99	0.767	0.388	0.357	0.714	0.662	0.971	0.788	0.295	0.590	0.284
	0.995	0.759	0.385	0.357	0.715	0.671	0.967	0.761	0.300	0.599	0.287
	1.00	0.716	0.358	0.358	0.716	0.716	0.962*	0.729*	0.306*	0.612*	0.290*

*Values evaluated by extrapolation from results for $(a_1+a_2)/r_{12} = 0.9$ to 0.995.

Table 6. The Droplet Mobility Parameters for the Slow Motion of Three Coaxial Identical Fluid Spheres ($a_1 = a_2 = a_3 = a$, $\eta_1^* = \eta_2^* = \eta_3^* = \eta^*$) with Equal Spacings ($r_{12} = r_{23} = d$)

η^*	$2a/d$	$M_{11}^{(p)}$	$M_{22}^{(p)}$	$M_{12}^{(p)}$	$M_{13}^{(p)}$	$M_{11}^{(n)}$	$M_{22}^{(n)}$	$M_{12}^{(n)}$	$M_{13}^{(n)}$
0.5	0.2	0.9998	0.9997	0.1163	0.0585	1.0000	1.0000	0.0585	0.0292
	0.4	0.9970	0.9944	0.2300	0.1189	1.0000	1.0000	0.1180	0.0585
	0.6	0.9845	0.9723	0.3380	0.1857	1.0000	1.0000	0.1795	0.0881
	0.8	0.9471	0.9127	0.4398	0.2684	1.0000	1.0001	0.2440	0.1184
	0.9	0.9035	0.8529	0.4926	0.3275	1.0002	1.0004	0.2777	0.1342
	0.95	0.8606	0.8021	0.5240	0.3737	1.0003	1.0006	0.2950	0.1424
	0.99	0.7784	0.7167	0.5627	0.4489	1.0004	1.0008	0.3091	0.1491
	1.00	0.6028	0.6028	0.6028	0.6028	1.0009	1.0010	0.3130	0.1513
1.0	0.2	0.9998	0.9996	0.1246	0.0627	1.0000	1.0000	0.0628	0.0313
	0.4	0.9963	0.9932	0.2452	0.1276	1.0000	1.0000	0.1270	0.0628
	0.6	0.9814	0.9669	0.3579	0.2000	0.9999	0.9998	0.1942	0.0946
	0.8	0.9379	0.8997	0.4621	0.2904	0.9994	0.9988	0.2660	0.1275
	0.9	0.8882	0.8354	0.5155	0.3563	0.9986	0.9973	0.3040	0.1448
	0.95	0.8402	0.7825	0.5468	0.4080	0.9978	0.9958	0.3235	0.1539
	0.99	0.7514	0.6997	0.5838	0.4914	0.9968	0.9937	0.3394	0.1615
	1.00	0.6140	0.6140	0.6140	0.6140	0.9966	0.9930	0.3432	0.1633
5.0	0.2	0.9997	0.9994	0.1408	0.0710	1.0000	1.0000	0.0713	0.0355
	0.4	0.9948	0.9904	0.2755	0.1452	1.0000	0.9999	0.1450	0.0712
	0.6	0.9743	0.9553	0.3978	0.2291	0.9995	0.9991	0.2237	0.1076
	0.8	0.9174	0.8732	0.5068	0.3369	0.9967	0.9935	0.3099	0.1453
	0.9	0.8545	0.8011	0.5610	0.4183	0.9918	0.9840	0.3570	0.1657
	0.95	0.7968	0.7470	0.5913	0.4818	0.9868	0.9740	0.3823	0.1769
	0.99	0.6870	0.6759	0.6229	0.5911	0.9794	0.9589	0.4039	0.1870
	1.00	0.6371	0.6371	0.6371	0.6371	0.976	0.952	0.409	0.190

respectively, are presented for three cases of relative radii. To avoid superfluity, here we do not list the values of the rotational mobility parameters for the case of three rigid spheres. Same as the collocation procedure employed in the previous section, rings at $\theta_i = \alpha$, $\pi/2 - \alpha$, $\pi/2 + \alpha$ and $\pi - \alpha$ on the surface of each sphere with $\alpha = 0.01° \sim 0.1°$ are taken to be the four basic multipoles and additional rings are chosen to divide the arc in a meridian plane into equal segments. For the most difficult case of a chain of touching spheres ($r_{12} = a_1 + a_2 = a_2 + a_3 = r_{23}$), the number of multipoles $K = 100$ is sufficiently large so that the interaction parameters converge to at least three figures after the decimal point. In general, the particle interactions increase with decreasing gap thickness between two neighboring spheres. Again, from Tables 4 and 5, it can be seen that $M_{21}^{(p,n)}/M_{12}^{(p,n)} = m_2/m_1$ for this symmetric case of three spheres, which demonstrates the correctness of the collocation solutions. In Table 6, the results of the mobility parameters for the case of three identical droplets with various internal-to-external viscosity ratios are given.

For the translation of three coaxial fluid spheres in the more general case, such as $a_1 \neq a_3$ and/or $r_{12} \neq r_{23}$, the numerical solutions of the droplet interactions can be obtained by the same collocation technique without any further difficulty. However, all eighteen interaction parameters, instead of ten for the symmetric case, are required to compute the droplet velocities.

It may be of interest to see how significantly the existence of a third droplet affects the mobilities of two neighboring droplets. In Figures 2 and 3, the normalized velocities of three identical spheres with equal spacings ($\eta_1^* = \eta_2^* = \eta_3^* = \eta^*$, $a_1 = a_2 = a_3 = a$, $r_{12} = r_{23} = d$) moving with equal applied forces in the directions parallel and perpendicular, respectively, to their line of centers are plotted by solid curves as a function of the separation parameter $2a/d$. For each curve, a value of η^* is selected. The corresponding velocities of the first and second spheres when the third sphere is not present are plotted by dashed curves in the same figures for comparison. It can be seen that the existence of the third sphere is to enhance the mobilities of the other two spheres. As expected, the enhancement in mobility in general is much more significant on sphere 2 than on sphere 1. For the motion of three spheres along their line of centers, the migration velocity of the central one is not a monotonic increasing function of $2a/d$, as illustrated in Figure 2b. When these spheres are touched with one another, Figures 2a and 2b exhibit that they have the same velocity and migrate as a single body. On the other hand, for the motion of three fluid spheres normal to their line of centers, the mobility of each sphere increases monotonically with the increase of $2a/d$, as shown in Figures 3a and 3b. The central sphere always translates faster than the end ones, even for the case of three touching spheres. For the motion of three solid spheres perpendicular to the line of centers, similar to the case of two solid spheres, the translational velocity of each sphere and the rotational velocity of each end sphere are not monotonic increasing functions of $2a/d$, as shown in Figures 3a, 3b, and 3c. Note that the central sphere does not rotate in this symmetric configuration. When the three solid spheres are touching, they migrate as a rigid body (without rotation) with $U_1 = U_2 = U_3 \simeq 1.60 U^{(0)}$.

To demonstrate the validity of our collocation scheme to the general three-dimensional problem, we have solved for the cases of three collinear identical droplets moving parallel or perpendicular to their line of centers but at an arbitrary orientation and inclination with respect to the xy-plane. $18K(2M-1)$ linear algebraic equations derived from Eqs. 13 were used to determine the equal-number coefficients for the flow field and the same procedure of selecting collocation rings was employed. Obviously, this problem can be reformulated as a one of those already solved with the solutions given in Table 6. A comparison between both results shows good agreement and presents evidence of successful collocation solution of a true general three-dimensional problem.

Solutions to the problem of linear chains consisting of 5, 7, 9, 11, 13, 15 and more identical spheres with equal spacings moving with equal applied forces have also been obtained by the collocation method. The results of the normalized velocities for chains containing N gas bubbles and rigid spheres ($N=1$, 3, 5, ..., 15) with $2a/d=0.5$ are plotted against the sphere number j in Figures 4 and 5, respectively. These velocities for the central spheres in an axisymmetrically translating chain of 101 bubbles or rigid spheres as well as in a transversally moving chain of 61 bubbles or 31 rigid spheres are also shown. Although the mobility has a discrete value for each sphere, the values have been connected by solid curves to indicate each individual chain. It can be seen that the translational velocity of the central sphere increases with the increase of the chain length. The relative mobility of adjacent spheres changes rapidly when the ends of a chain are approached; this demonstrates the importance of end effects. As the length of the chain increases, the velocity of the central spheres in the chain changes very slowly. In the limit of an infinite chain the velocity of each sphere would be the same. The broken curves in Figures 4 and 5 indicate the change in mobility of the jth sphere in a chain as more spheres are added to the chain. These curves tend to become horizontal as the chain length increases. Corresponding figures to Figures 5a, 5b, and 5c for the normalized translational and rotational drag coefficients of chains of identical rigid spheres with equal spacings were provided by Ganatos et al. (1978).

Figure 6 represents plots of the normalized migration velocities vs. the sphere number in a chain containing 9 identical and equally spaced fluid spheres with $2a/d=0.5$ at various values of relative viscosity η^*. These results demonstrate that as the internal-to-external viscosity ratio increases the normalized mobility of each sphere in the chain will be increased. The particle interaction is strongest for a chain of rigid spheres ($\eta^* \to \infty$) and weakest for an equivalent chain of gas bubbles ($\eta^* \to 0$).

The results in Figures 4-6 apply only to the case of $2a/d=0.5$. In order to determine the effect of sphere spacing on the droplet mobility, curves of the normalized migration velocity vs. the sphere number with $2a/d$ as a parameter are plotted for a chain of 9 spheres in Figure 7. Only the limiting cases of a gas bubble chain and a solid sphere chain are shown. The results in Figure 7 indicate that the end effects will decrease as the spacing increases. Also, when the spheres get closer together the mobility of each sphere in the chain is increased. Note that, for the case of a finite chain of touching spheres translating along their line of centers, the velocities of all spheres are equal. However, for the movement of a chain of touching fluid spheres perpendicular to their line of centers, the velocities of the spheres can still be different from one another.

It can be found from the results in Tables 1-6 and Figures 2-7 that the particle interactions in a chain of droplets translating along their line of centers are always stronger than those for an identical chain moving normal to their line of centers.

Average Settling Velocity in a Suspension of Droplets

In practical applications of sedimentation phenomena, collections of droplets in bounded systems (say, in a container filled with an emulsion) are usually encountered. It is therefore necessary to determine the dependence of the average settling velocity in a suspension on the volume fraction of droplets. Based on a microscopic model of particle interactions in a dilute dispersion which involves both statistical and low Reynolds number hydrodynamic concepts (Batchelor, 1972), the mean settling velocity of type i droplets (having radius a_i and volume fraction φ_i) in a bounded suspension of droplets that

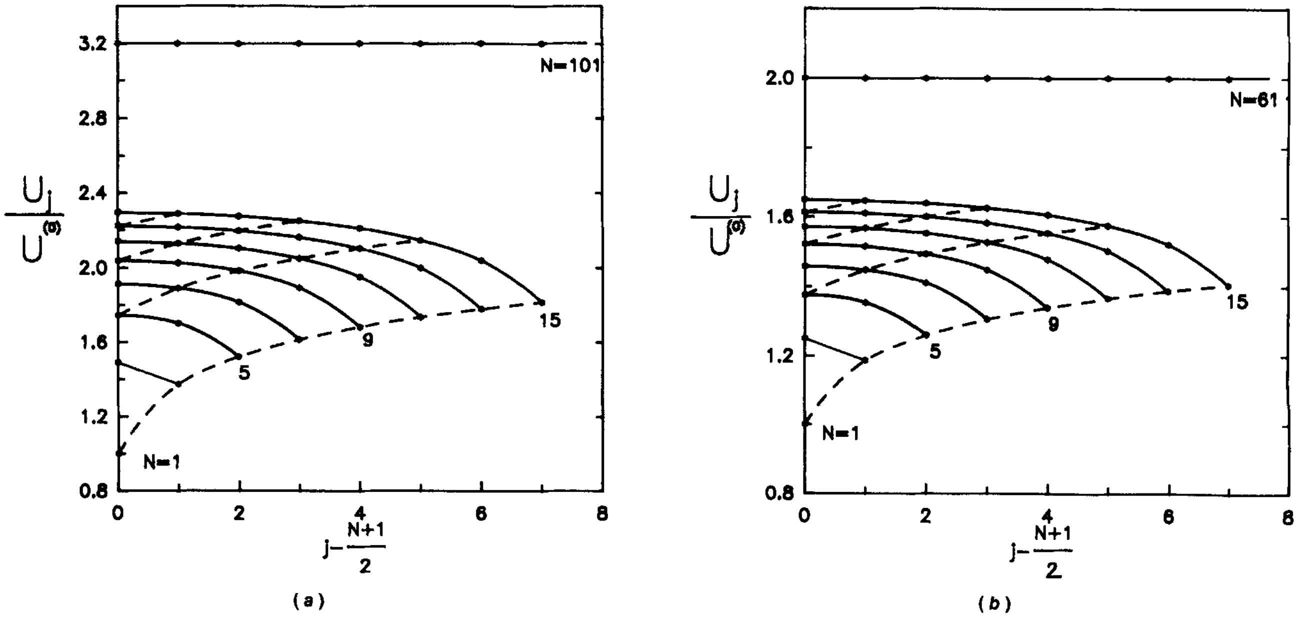

Figure 4. Normalized migration velocities for chains containing N identical and equally spaced gas bubbles ($\eta^*=0$) with $2a/d=0.5$ moving with equal applied forces vs. the sphere number j: (a) migration parallel to the line of bubble centers; (b) migration perpendicular to the line of bubble centers.

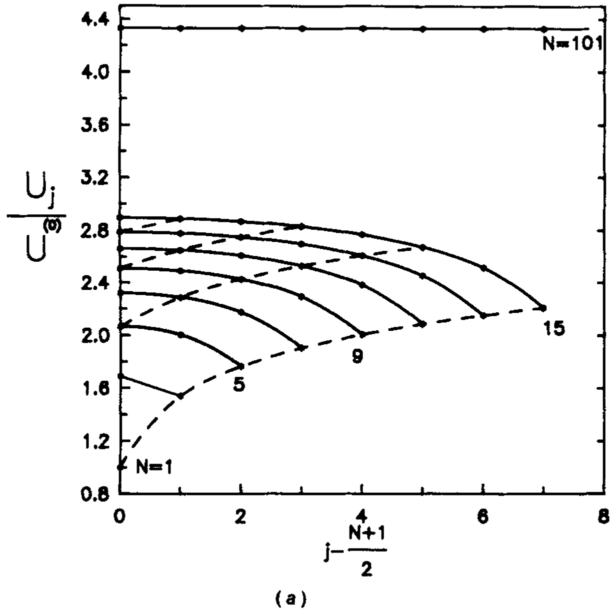

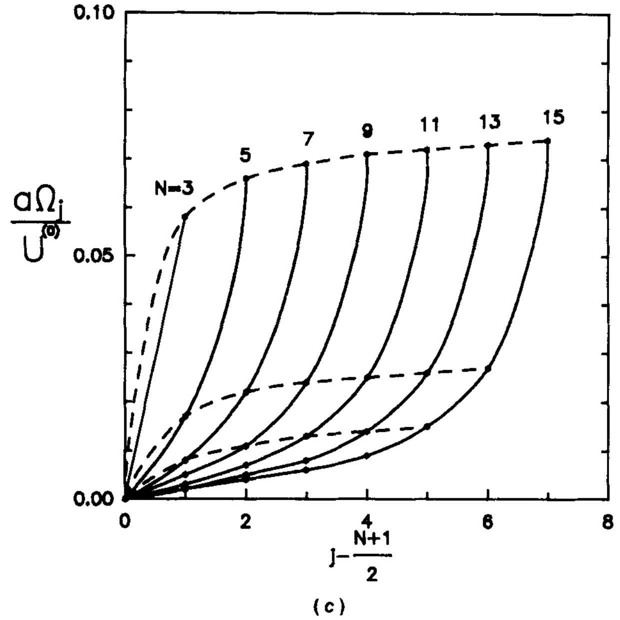

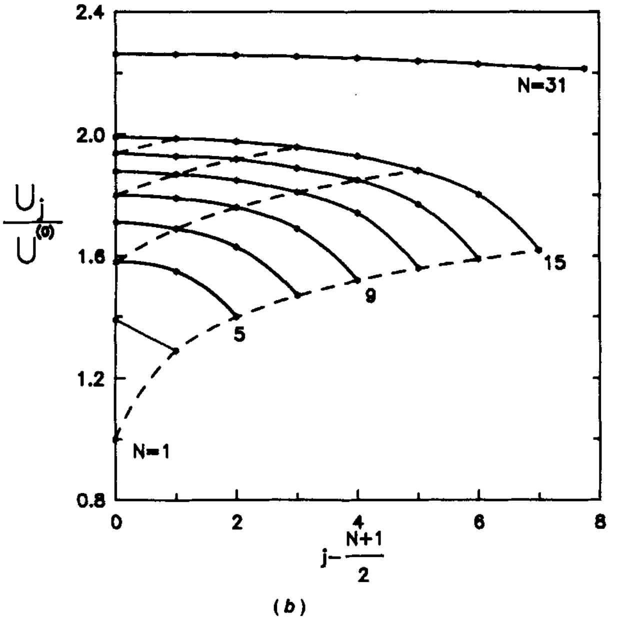

Figure 5. Normalized particle velocities for chains containing N identical and equally spaced rigid spheres ($\eta^* \rightarrow \infty$) with $2a/d = 0.5$ moving with equal applied forces vs. the sphere number j: (a) migration parallel to the line of particle centers; (b) and (c) migration (with free rotation) perpendicular to the line of particle centers.

have the same physical properties can be expressed as (Reed and Anderson, 1980)

$$\langle \underline{U}_i \rangle = \underline{U}_i^{(0)}\left[1 + \sum_j \nu_{ij}\varphi_j + O(\varphi^2)\right] \tag{30}$$

with

$$\nu_{ij} = -\left[1 + 2\lambda\frac{a_j}{a_i} + \left(\frac{a_j}{a_i}\right)^2\right] + \left(1 + \frac{a_i}{a_j}\right)^3 \int_0^1 \left\{[M_{11}^{(p)} + 2M_{11}^{(n)} - 3] + \left(\frac{a_j}{a_i}\right)^2\left[M_{12}^{(p)} + 2M_{12}^{(n)} - \frac{2\lambda\omega}{1 + a_i/a_j}\right]\right\}\omega^{-4}d\omega \tag{31}$$

where

$$\varphi = \sum_j \varphi_j \tag{32}$$

$$\lambda = \frac{1 + (3/2)\eta^*}{1 + \eta^*} \tag{33}$$

$$\omega = \frac{a_1 + a_2}{r_{12}} \tag{34}$$

$M_{11}^{(p)}$, $M_{12}^{(p)}$, $M_{11}^{(n)}$ and $M_{12}^{(n)}$ are the two-particle mobility parameters defined by Eq. 25, and subscripts 1 and 2 represent types i and j droplets respectively. In the derivation of Eq. 31,

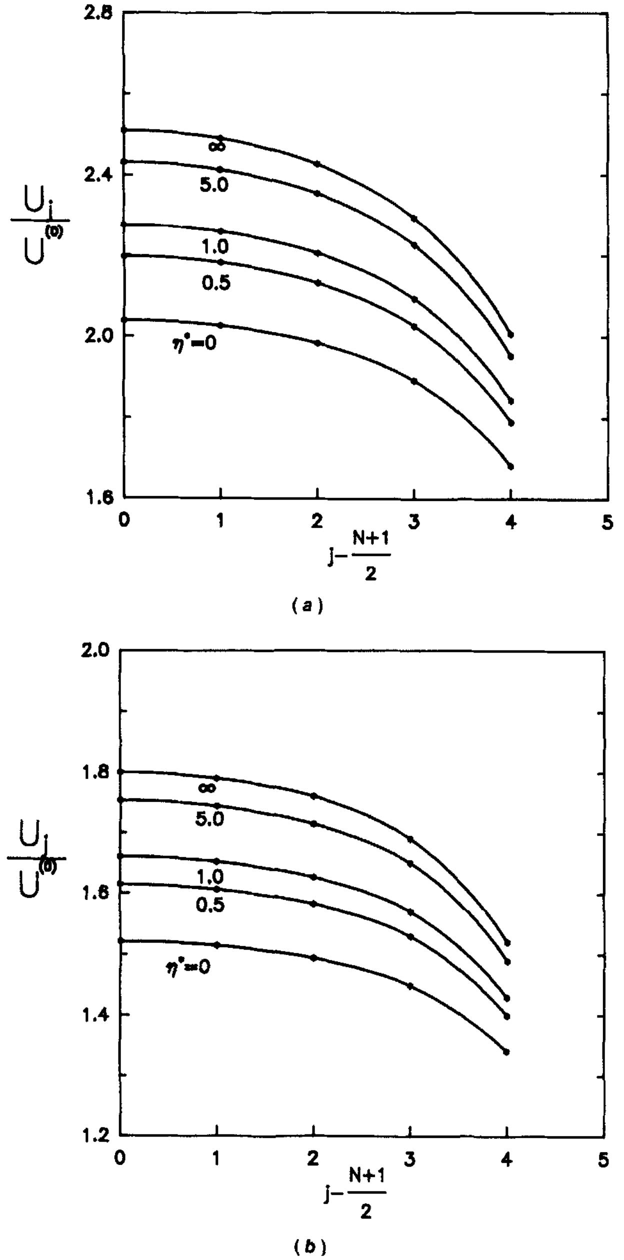

Figure 6. Normalized migration velocities for chains consisting of nine identical and equally spaced droplets with $2a/d=0.5$ moving with equal applied forces at different internal-to-external viscosity ratios: (a) migration parallel to the line of droplet centers; (b) migration (with free rotation for the case of $\eta^*\to\infty$) perpendicular to the line of droplet centers.

it has been assumed that the droplets interact by a hard sphere potential (without long range energy) and the two-particle radial distribution function has its equilibrium value. The mean settling velocities are calculated for a reference frame in which the net flux of the droplets and the surrounding fluid is zero.

The numerical results of the integrand in Eq. 31 as a function of ω for a suspension of identical droplets with various values of η^* computed from the solution of two-droplet interaction parameters are exhibited in Table 7. The integration can be performed numerically using these data, and the results of the interaction coefficient ν_{ij} for a suspension of droplets with the same viscosity at various values of η^* and a_j/a_i are presented in Table 8. Note that coefficient ν_{ij} is negative and its magnitude increases monotonically with the increase of η^* or a_j/a_i. All the previous calculations of ν_{ij} (Batchelor, 1972; Reed and Anderson, 1980; Haber and Hetsroni, 1981) for a suspension of identical solid or fluid spheres using approximations for the mobility parameters of two near-contact spheres, as also listed and compared with the exact results in Table 8, are found to slightly overestimate the effect of particles' volume fraction on the average particle velocity.

Table 7. Numerical Values of the Integrand in Eq. 31 as a function of ω for a Suspension of Identical Droplets with Various Values of η^*

	$-\{[M_{11}^{(p)}+2M_{11}^{(n)}-3]+[M_{12}^{(p)}+2M_{12}^{(n)}-\lambda\omega]\}\omega^{-4}$				
ω	$\eta^*=0$	$\eta^*=0.5$	$\eta^*=1.0$	$\eta^*=5.0$	$\eta^*=\infty$
0.1	0.0600	0.0970	0.1400	0.1967	0.2400
0.2	0.0631	0.1090	0.1356	0.1971	0.2369
0.3	0.0632	0.1079	0.1338	0.1925	0.2285
0.4	0.0633	0.1062	0.1304	0.1850	0.2195
0.5	0.0640	0.1031	0.1252	0.1746	0.2032
0.6	0.0625	0.0985	0.1177	0.1607	0.1882
0.7	0.0612	0.0921	0.1082	0.1446	0.1674
0.8	0.0593	0.0841	0.0972	0.1282	0.1492
0.9	0.0556	0.0750	0.0860	0.1147	0.1357
0.95	0.0530	0.0703	0.0809	0.1108	0.1321
0.96	0.0523	0.0691	0.0802	0.1102	0.1323
0.97	0.0517	0.0684	0.0794	0.1103	0.1327
0.98	0.0511	0.0677	0.0786	0.1105	0.1340
0.99	0.0504	0.0667	0.0781	0.1114	0.1367
0.995	0.0501	0.0659	0.0777	0.1124	0.1398
0.999	0.0500	0.0662	0.0777	0.1121	0.1429
1.0	0.0494	0.0655	0.0774	0.1127	0.1894

Summary

In this work the motion of a finite assemblage of spherical droplets in an arbitrary configuration has been studied by a combined analytical-numerical method. The spheres may differ in size, in viscosity and in migration velocity. A collocation technique has been used to obtain the numerical solutions for the velocity field in each fluid phase. The results for the droplet

Table 8. The Results of Coefficient ν_{ij} for a Suspension of Droplets with the Same Viscosity at Various Values of η^* and a_j/a_i

	$-\nu_{ij}$				
a_j/a_i	$\eta^*=0$	$\eta^*=0.5$	$\eta^*=1.0$	$\eta^*=5.0$	$\eta^*=\infty$
0.5	2.27	3.41	3.80	4.65	5.01
1.0	4.44	5.07	5.41	6.10	6.49
2.0	9.06	9.89	10.15	11.46	11.86
1.0*	—	—	—	—	6.55
1.0**	4.54	5.17	5.50	6.18	6.53
1.0†	4.49	(5.1)	(5.5)	(6.2)	6.59

*Results of Batchelor (1972).
**Results of Reed and Anderson (1980).
†Results of Haber and Hetsroni (1981).
Values in parentheses are read from a figure.

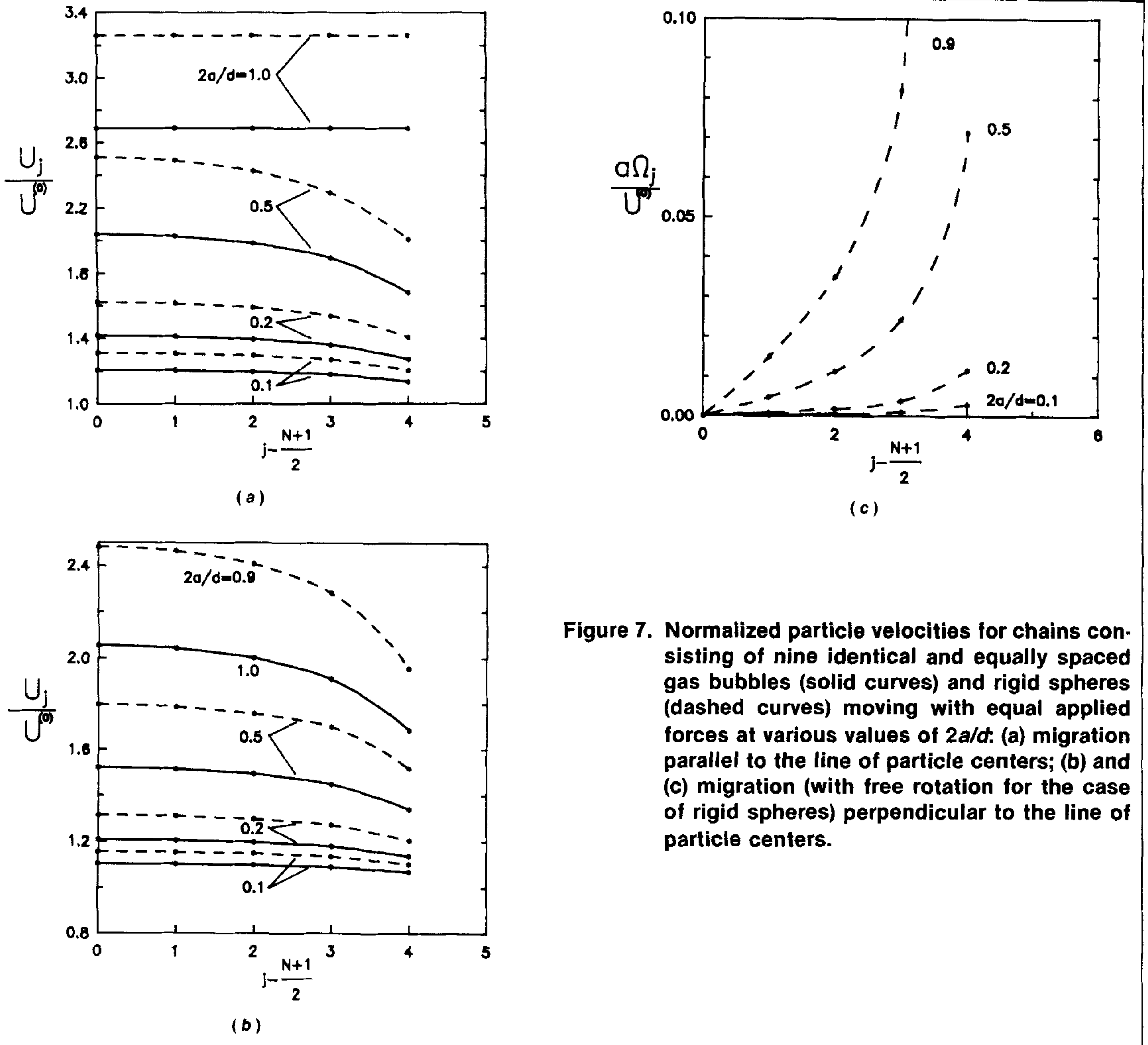

Figure 7. Normalized particle velocities for chains consisting of nine identical and equally spaced gas bubbles (solid curves) and rigid spheres (dashed curves) moving with equal applied forces at various values of $2a/d$: (a) migration parallel to the line of particle centers; (b) and (c) migration (with free rotation for the case of rigid spheres) perpendicular to the line of particle centers.

interaction parameters indicate that the solution procedure converges rapidly and solutions can be obtained to any desired degree of accuracy for various cases even when the spheres are touching one another or the number of spheres is quite large.

In the second section, the linear algebraic formulae to solve the problem of slow motion of multiple spheres were derived and the procedure of the application of the collocation technique was given. The numerical results to correct the Hadamard-Rybczynski equation 1 for the two-sphere and linearly multiple-sphere systems were obtained for various cases in the third and fourth sections respectively. It has been found that the particle velocities for the asymmetric motion of a chain of touching fluid spheres can be different from one another, although these spheres always migrate as a single body in an axisymmetric motion. In the fifth section, the 'exact' solutions for the hydrodynamic interactions between two droplets were utilized to calculate the mean settling velocity in a bounded dispersion of small solid or fluid spheres.

Acknowledgment

This research was supported by the National Science Council of the Republic of China under Grant NSC81-0402-E002-03.

Appendix A: Formulation for the Axisymmetric Motion of a String of Droplets

In this appendix we consider the translation of a chain of N spherical droplets in an unbounded, immiscible fluid at rest at infinity parallel to their line of centers (along the z axis). Here, the origin of the circular cylindrical coordinate system (ρ, ϕ, z) is taken at the center of the first sphere. The droplets may differ in radius, in migration velocity, and in physical properties, and they are allowed to be unequally spaced.

The fluid velocities inside and outside the droplets are governed by Eqs. 2 or the fourth-order differential equation for axisymmetric creeping flow:

$$E^4\Psi = E^2(E^2\Psi) = 0 \quad \text{(A1a)}$$

$$E^4\Psi_i = 0, \quad i = 1, 2, \ldots, N \quad \text{(A1b)}$$

where Ψ_i and Ψ are the Stokes stream functions for the flow inside droplet i and for the external flow, respectively. The operator E^2 has the following form in spherical coordinates (r, θ, ϕ):

$$E^2 = \frac{\partial^2}{\partial r^2} + \frac{\sin\theta}{r^2}\frac{\partial}{\partial\theta}\left(\frac{1}{\sin\theta}\frac{\partial}{\partial\theta}\right). \quad \text{(A2)}$$

In circular cylindrical coordinates, the stream function Ψ (or Ψ_i) is related to the components of the velocity field $\underline{v}$ (or $\underline{v}_i$) by the formulae

$$v_\rho = \frac{1}{\rho}\frac{\partial\Psi}{\partial z} \quad \text{(A3a)}$$

$$v_z = -\frac{1}{\rho}\frac{\partial\Psi}{\partial\rho}. \quad \text{(A3b)}$$

The boundary conditions for the velocity field at the droplet interfaces and far away from the droplets are given by Eqs. 3, in which $\underline{U}_i = U_i\underline{e}_z$.

A sufficiently general solution to Eqs. A1 is

$$\Psi = \sum_{j=1}^{N}\sum_{n=2}^{\infty}[\beta_{jn}r_j^{-n+1} + \delta_{jn}r_j^{-n+3}]G_n^{-1/2}(\mu_j) \quad \text{(A4a)}$$

$$\Psi_i = \sum_{n=2}^{\infty}[\alpha_{in}r_i^n + \gamma_{in}r_i^{n+2}]G_n^{-1/2}(\mu_i), \quad i = 1, 2, \ldots, N \quad \text{(A4b)}$$

where $G_n^{-1/2}(\mu_i)$ is the Gegenbauer polynomial of order n and degree $-1/2$ and μ_i is used to denote $\cos\theta_i$. The Gegenbauer polynomials are related to Legendre polynomials via the relation

$$G_n^{-1/2}(\mu) = \frac{P_{n-2}(\mu) - P_n(\mu)}{2n-1}. \quad \text{(A5)}$$

A solution in the form of Eqs. A4 immediately satisfies boundary condition 3d and the requirement of finite velocity in the interior of each droplet. The unknown coefficients β_{jn}, δ_{jn}, α_{in} and γ_{in} are to be determined using the boundary conditions at the droplet interfaces.

Application of Eqs. A3 to Eqs. A4 leads to the components of fluid velocities $\underline{v}$ and $\underline{v}_i$:

$$v_\rho = \sum_{j=1}^{N}\sum_{n=2}^{\infty}[\beta_{jn}\beta_n'(r_j, \mu_j) + \delta_{jn}\delta_n'(r_j, \mu_j)] \quad \text{(A6a)}$$

$$v_z = \sum_{j=1}^{N}\sum_{n=2}^{\infty}[\beta_{jn}\beta_n''(r_j, \mu_j) + \delta_{jn}\delta_n''(r_j, \mu_j)] \quad \text{(A6b)}$$

$$v_{i\rho} = \sum_{n=2}^{\infty}[\alpha_{in}\alpha_n'(r_i, \mu_i) + \gamma_{in}\gamma_n'(r_i, \mu_i)] \quad \text{(A6c)}$$

$$v_{iz} = \sum_{n=2}^{\infty}[\alpha_{in}\alpha_n''(r_i, \mu_i) + \gamma_{in}\gamma_n''(r_i, \mu_i)] \quad \text{(A6d)}$$

where

$$\beta_n'(r_j, \mu_j) = -(n+1)r_j^{-n-1}(1-\mu_j^2)^{-1/2}G_{n+1}^{-1/2}(\mu_j) \quad \text{(A7a)}$$

$$\delta_n'(r_j, \mu_j) = -r_j^{-n+1}(1-\mu_j^2)^{-1/2}[(n+1)G_{n+1}^{-1/2}(\mu_j) - 2\mu_j G_n^{-1/2}(\mu_j)] \quad \text{(A7b)}$$

$$\beta_n''(r_j, \mu_j) = -r_j^{-n-1}P_n(\mu_j) \quad \text{(A7c)}$$

$$\delta_n''(r_j, \mu_j) = -r_j^{-n+1}[P_n(\mu_j) + 2G_n^{-1/2}(\mu_j)] \quad \text{(A7d)}$$

$$\alpha_n'(r_i, \mu_i) = -r_i^{n-2}(1-\mu_i^2)^{-1/2}[(n+1)G_{n+1}^{-1/2}(\mu_i) - (2n-1)\mu_i G_n^{-1/2}(\mu_i)] \quad \text{(A7e)}$$

$$\gamma_n'(r_i, \mu_i) = -r_i^n(1-\mu_i^2)^{-1/2}[(n+1)G_{n+1}^{-1/2}(\mu_i) - (2n+1)\mu_i G_n^{-1/2}(\mu_i)] \quad \text{(A7f)}$$

$$\alpha_n''(r_i, \mu_i) = -r_i^{n-2}[P_n(\mu_i) + (2n-1)G_n^{-1/2}(\mu_i)] \quad \text{(A7g)}$$

$$\gamma_n''(r_i, \mu_i) = -r_i^n[P_n(\mu_i) + (2n+1)G_n^{-1/2}(\mu_i)]. \quad \text{(A7h)}$$

Utilizing the relations

$$\frac{\partial}{\partial r_i} = (1-\mu_i^2)^{1/2}\frac{\partial}{\partial\rho} + \mu_i\frac{\partial}{\partial z} \quad \text{(A8a)}$$

$$\frac{\partial}{\partial\mu_i} = -r_i\mu_i(1-\mu_i^2)^{-1/2}\frac{\partial}{\partial\rho} + r_i\frac{\partial}{\partial z} \quad \text{(A8b)}$$

and the recurrence relations of the Legendre and Gegenbauer polynomials, one can apply the boundary conditions 3a to 3c along the interface of each droplet to Eqs. A6 to yield

$$\sum_{j=1}^{N}\sum_{n=2}^{\infty}\{\beta_{jn}[(1-\mu_i^2)^{1/2}\beta_n'(r_j, \mu_j) + \mu_i\beta_n''(r_j, \mu_j)] + \delta_{jn}[(1-\mu_i^2)^{1/2}\delta_n'(r_j, \mu_j) + \mu_i\delta_n''(r_j, \mu_j)]\}_{r_i=a_i} = \mu_i U_i \quad \text{(A9a)}$$

$$\sum_{j=1}^{N}\sum_{n=2}^{\infty}\{\beta_{jn}\beta_n'(r_j, \mu_j) + \delta_{jn}\delta_n'(r_j, \mu_j)\}_{r_i=a_i} - \sum_{n=2}^{\infty}\{\alpha_{in}\alpha_n'(a_i, \mu_i) + \gamma_{in}\gamma_n'(a_i, \mu_i)\} = 0 \quad \text{(A9b)}$$

$$\sum_{j=1}^{N}\sum_{n=2}^{\infty}\{\beta_{jn}\beta_n''(r_j, \mu_j) + \delta_{jn}\delta_n''(r_j, \mu_j)\}_{r_i=a_i} - \sum_{n=2}^{\infty}\{\alpha_{in}\alpha_n''(a_i, \mu_i) + \gamma_{in}\gamma_n''(a_i, \mu_i)\} = 0 \quad \text{(A9c)}$$

$$\sum_{j=1}^{N}\sum_{n=2}^{\infty}\{\beta_{jn}[(2\mu_i^2-1)\beta_n^*(r_j, \mu_j) + 2\mu_i(1-\mu_i^2)^{1/2}\beta_n^{**}(r_j, \mu_j)] + \delta_{jn}[(2\mu_i^2-1)\delta_n^*(r_j, \mu_j) + 2\mu_i(1-\mu_i^2)^{1/2}\delta_n^{**}(r_j, \mu_j)]\}_{r_i=a_i} - \eta_i^*\sum_{n=2}^{\infty}\{\alpha_{in}\alpha_n^*(a_i, \mu_i) + \gamma_{in}\gamma_n^*(a_i, \mu_i)\} = 0 \quad \text{(A9d)}$$

where

$$\beta_n^*(r_j,\ \mu_j) = r_j^{-n-2}(1-\mu_j^2)^{1/2}[2(n+1)P_n(\mu_j) + 2\mu_j P_n'(\mu_j)] \quad \text{(A10a)}$$

$$\beta_n^{**}(r_j,\ \mu_j) = r_j^{-n-2}[(2n+1)(n+1)G_{n+1}^{-1/2}(\mu_j) - 2(n+1)\mu_j P_n(\mu_j) + \frac{1}{n}\mu_j^2 P_n'(\mu_j)] \quad \text{(A10b)}$$

$$\delta_n^*(r_j,\ \mu_j) = r_j^{-n}(1-\mu_j^2)^{1/2}[2nP_n(\mu_j) + 2nG_n^{-1/2}(\mu_j) - 4\mu_j P_{n-1}(\mu_j) + \frac{2(n-1)}{n}P_n'(\mu_j) - \frac{2(n-2)}{n(n-1)}\mu_j^2 P_{n-1}'(\mu_j)] \quad \text{(A10c)}$$

$$\delta_n^{**}(r_j,\ \mu_j) = r_j^{-n}[(2n-1)(n+1)G_{n+1}^{-1/2}(\mu_j) + 2(2\mu_j^2-1)P_{n-1}(\mu_j) - 2(2n-1)\mu_j G_n^{-1/2}(\mu_j) - 2n\mu_j P_n(\mu_j) + \frac{1}{n}\mu_j^2 P_n'(\mu_j) - \frac{2}{n(n-1)}\mu_j^3 P_{n-1}'(\mu_j)] \quad \text{(A10d)}$$

$$\alpha_n^*(r_i,\ \mu_i) = r_i^{n-3}(1-\mu_i^2)^{1/2}\left[\frac{3}{n}\mu_i P_n'(\mu_i) - 3P_n(\mu_i) + (n-3)(2n-1)G_n^{-1/2}(\mu_i) + \frac{(n-3)(2n-1)}{n(n-1)}\mu_i^2 P_{n-1}'(\mu_i)\right] \quad \text{(A10e)}$$

$$\gamma_n^*(r_i,\ \mu_i) = r_i^{n-1}(1-\mu_i^2)^{1/2}\left[\frac{1}{n}\mu_i P_n'(\mu_i) - P_n(\mu_i) + (n-1)(2n+1)G_n^{-1/2}(\mu_i) + \frac{(2n+1)}{n}\mu_i^2 P_{n-1}'(\mu_i)\right] \quad \text{(A10f)}$$

$\eta_i^* = \eta_i/\eta$, and $i = 1, 2, \ldots,$ or N. The prime on $P_n(\mu_i)$ means differentiation with respect to μ_i.

The multipole collocation method (Gluckman et al., 1971) enforces the boundary conditions at K discrete values of θ_i on the interface of each droplet and truncates the infinite series in Eqs. A4 and A9 into finite ones with K terms each. For N droplets in the chain, this results in a set of $4KN$ simultaneous linear algebraic equations for the $4KN$ unknown coefficients β_{jn}, δ_{jn}, α_{in} and γ_{in} of the truncated solution. These equations can be solved using any standard matrix-reduction technique.

The force exerted by the external fluid on the spherical boundary $r_i = a_i$ can be determined from (Happel and Brenner, 1983)

$$F_i = \eta\pi\int_0^\pi r_i^3\sin^3\theta_i \frac{\partial}{\partial r_i}\left(\frac{E^2\Psi}{r_i^2\sin^2\theta_i}\right) r_i d\theta_i. \quad \text{(A11)}$$

Substitution of Eq. A4a into the above integral and application of the orthogonality properties of the Gegenbauer polynomials result in the simple relation

$$F_i = 4\pi\eta\delta_{i2} \quad \text{(A12)}$$

where $i = 1, 2, \ldots,$ or N. This equation shows that only the first multipole contributes to the drag force exerted on the droplet.

Appendix B: Formulation for the Slow Motion of Multiple Rigid Spheres

For the three-dimensional motion of N rigid spheres in an immense, quiescent fluid as illustrated in Figure 1, only the flow field of the surrounding fluid phase needs to be considered. The boundary conditions for the fluid velocity at the particle surfaces are

$$r_i = a_i: \quad \underline{v} = \underline{U}_i + \underline{\Omega}_i \times a_i \underline{e}_{ri} \quad \text{(B1)}$$

instead of Eqs. 3a to 3c, for $i = 1, 2, \ldots,$ or N. Here, $\underline{\Omega}_i$ is the angular velocity of sphere i and can be written as $\Omega_{ix}\underline{e}_x + \Omega_{iy}\underline{e}_y + \Omega_{iz}\underline{e}_z$. Applying Eq. B1 to Eq. 10a and employing the truncation procedure to result in Eqs. 13, one obtains

$$\sum_{j=1}^{N}\sum_{m=0}^{M-1}\sum_{\substack{n=m\\ n\neq 0}}^{m+K-1}[A_{jmn}A_{jimn}^{(1)} + B_{jmn}B_{jimn}^{(1)} + \ldots + F_{jmn}F_{jimn}^{(1)}]_{r_i=a_i} = U_{ix}(1-\mu_i^2)^{1/2}\cos\phi_i + U_{iy}(1-\mu_i^2)^{1/2}\sin\phi_i + U_{iz}\mu_i \quad \text{(B2a)}$$

$$\sum_{j=1}^{N}\sum_{m=0}^{M-1}\sum_{\substack{n=m\\ n\neq 0}}^{m+K-1}[A_{jmn}A_{jimn}^{(2)} + B_{jmn}B_{jimn}^{(2)} + \ldots + F_{jmn}F_{jimn}^{(2)}]_{r_i=a_i} = U_{ix}\mu_i\cos\phi_i + U_{iy}\mu_i\sin\phi_i - U_{iz}(1-\mu_i^2)^{1/2} - a_i(\Omega_{ix}\sin\phi_i - \Omega_{iy}\cos\phi_i) \quad \text{(B2b)}$$

$$\sum_{j=1}^{N}\sum_{m=0}^{M-1}\sum_{\substack{n=m\\ n\neq 0}}^{m+K-1}[A_{jmn}A_{jimn}^{(3)} + B_{jmn}B_{jimn}^{(3)} + \ldots + F_{jmn}F_{jimn}^{(3)}]_{r_i=a_i} = -U_{ix}\sin\phi_i + U_{iy}\cos\phi_i - a_i[\Omega_{ix}\mu_i\cos\phi_i + \Omega_{iy}\mu_i\sin\phi_i - \Omega_{iz}(1-\mu_i^2)^{1/2}] \quad \text{(B2c)}$$

for $i = 1, 2, \ldots,$ or N. The $3NK(2M-1)$ unknown constants A_{jmn}, B_{jmn}, $\ldots$, and F_{jmn} in Eqs. B2 can be solved by using the boundary collocation technique described in the second section.

For the case of planar symmetry, that is, the centers of all the spheres lie in the plane $y=0$, $U_{iy} = \Omega_{ix} = \Omega_{iz} = 0$ and the constants A_{jmn}, D_{jmn} and F_{jmn} are all zero. Also, as discussed in the second section, two special cases can be deduced from the planar case. The fluid velocity field about a finite chain of spheres translating along their line of centers is axially symmetric and was solved by Gluckman et al. (1971). For the case of a string of spheres moving normal to their line of centers (the centers of all spheres lie on the z-axis and $U_{iz}=0$), Eqs. B2 can be simplified to

$$\sum_{j=1}^{N}\sum_{n=1}^{K}[B_{j1n}B_{jin}'(a_i,\ \mu_i) + C_{j1n}C_{jin}'(a_i,\ \mu_i) + E_{j1n}E_{jin}'(a_i,\ \mu_i)] = U_{ix}(1-\mu_i^2)^{1/2} \quad \text{(B3a)}$$

$$\sum_{j=1}^{N}\sum_{n=1}^{K}[B_{j1n}B''_{\rm jin}(a_i,\mu_i)+C_{j1n}C''_{\rm jin}(a_i,\mu_i)$$

$$+E_{j1n}E''_{\rm jin}(a_i,\mu_i)]=U_{ix}\mu_i+a_i\Omega_{iy} \quad \text{(B3b)}$$

$$\sum_{j=1}^{N}\sum_{n=1}^{K}[B_{j1n}B'''_{\rm jin}(a_i,\mu_i)+C_{j1n}C'''_{\rm jin}(a_i,\mu_i)$$

$$+E_{j1n}E'''_{\rm jin}(a_i,\mu_i)]=-U_{ix}-a_i\Omega_{iy}\mu_i \quad \text{(B3c)}$$

where the nine functions $B'_{\rm jin}(r_i,\mu_i)$, $C'_{\rm jin}(r_i,\mu_i)$, . . . , and $E'''_{\rm jin}(r_i,\mu_i)$ are defined by Eqs. C7 to C15 and the dependence on ϕ factors out. One can apply Eqs. B3 at K discrete values of θ_i along the surface of each sphere and generate a set of $3NK$ linear algebraic equations for the equal number of unknown coefficients B_{j1n}, C_{j1n} and E_{j1n}.

The hydrodynamic torque experienced by the sphere i about its center is given by (Happel and Brenner, 1983)

$$\underline{T}_i=-8\pi\eta\nabla[r_i^3\chi_{-2}^{(i)}],\quad i=1,2,\ldots,N \quad \text{(B4)}$$

while the drag force on the sphere is given by Eq. 15. Substitution of Eq. 6a into Eq. B4 yields

$$\underline{T}_i=-8\pi\eta(A_{i11}\underline{e}_x+B_{i11}\underline{e}_y+A_{i01}\underline{e}_z),\quad i=1,2,\ldots,N. \quad \text{(B5)}$$

The six coefficients for each of the N spheres in Eqs. 16 and B5 are known from the solution of Eqs. B2.

In a resistance problem, the results of the drag force and torque on each sphere can be expressed as

$$\underline{F}_i=\sum_{j=1}^{N}[\underline{\underline{K}}_{ij}\cdot\underline{F}_j^{(0)}+\frac{1}{a_i}\overline{\underline{\underline{P}}}_{ij}\cdot\underline{T}_j^{(0)}] \quad \text{(B6a)}$$

$$\underline{T}_i=\sum_{j=1}^{N}[a_i\underline{\underline{P}}_{ij}\cdot\underline{F}_j^{(0)}+\underline{\underline{R}}_{ij}\cdot\underline{T}_j^{(0)}] \quad \text{(B6b)}$$

for $i=1, 2, \ldots,$ or N, with

$$\underline{F}_j^{(0)}=-6\pi\eta a_j\underline{U}_j \text{ and } \underline{T}_j^{(0)}=-8\pi\eta a_j^3\underline{\Omega}_j \quad \text{(B7a,b)}$$

which are the force and torque exerted by the fluid on the jth sphere in the absence of all the other ones. The dimensionless resistance tensors $\underline{\underline{K}}_{ij}$, $\underline{\underline{R}}_{ij}$, $\underline{\underline{P}}_{ij}$ and $\overline{\underline{\underline{P}}}_{ij}$ are functions of the relative sizes, orientations and separation distances of the spheres. When the sphere i is infinitely separated from all of the other spheres,

$$\underline{\underline{K}}_{ii}=\underline{\underline{R}}_{ii}=\underline{\underline{I}},\quad \underline{\underline{K}}_{ij}=\underline{\underline{R}}_{ij}=\underline{\underline{0}}$$

$$(j=1,2,\ldots,N \text{ but } j\neq i) \quad \text{(B8a,b)}$$

$$\underline{\underline{P}}_{ij}=\overline{\underline{\underline{P}}}_{ij}=\underline{\underline{0}}\quad (j=1,2,\ldots,N) \quad \text{(B8c)}$$

for $i=1, 2, \ldots,$ or N.

In a mobility problem, the results of the particle velocities can be expressed as

$$\underline{U}_i=\sum_{j=1}^{N}[\underline{\underline{M}}_{ij}\cdot\underline{U}_j^{(0)}+a_i\overline{\underline{\underline{Q}}}_{ij}\cdot\underline{\Omega}_j^{(0)}] \quad \text{(B9a)}$$

$$\underline{\Omega}_i=\sum_{j=1}^{N}\left[\frac{1}{a_i}\underline{\underline{Q}}_{ij}\cdot\underline{U}_j^{(0)}+\underline{\underline{N}}_{ij}\cdot\underline{\Omega}_j^{(0)}\right] \quad \text{(B9b)}$$

for $i=1, 2, \ldots,$ or N, with

$$\underline{U}_j^{(0)}=-\frac{1}{6\pi\eta a_j}\underline{F}_j \text{ and } \underline{\Omega}_j^{(0)}=-\frac{1}{8\pi\eta a_j^3}\underline{T}_j \quad \text{(B10a,b)}$$

which are the translational and angular velocities of the sphere j subject to an applied force $-\underline{F}_j$ and torque $-\underline{T}_j$ in the absence of the other spheres. The dimensionless mobility tensors $\underline{\underline{M}}_{ij}$, $\underline{\underline{N}}_{ij}$, $\underline{\underline{Q}}_{ij}$ and $\overline{\underline{\underline{Q}}}_{ij}$ are also functions of the relative orientations, sizes and separation distances of the spheres. When the ith sphere is separated by an infinite distance from all of the others,

$$\underline{\underline{M}}_{ii}=\underline{\underline{N}}_{ii}=\underline{\underline{I}},\quad \underline{\underline{M}}_{ij}=\underline{\underline{N}}_{ij}=\underline{\underline{0}}$$

$$(j=1,2,\ldots,N \text{ but } j\neq i) \quad \text{(B11a,b)}$$

$$\underline{\underline{Q}}_{ij}=\overline{\underline{\underline{Q}}}_{ij}=\underline{\underline{0}}\quad (j=1,2,\ldots,N) \quad \text{(B11c)}$$

for $i=1, 2, \ldots,$ or N.

Appendix C

For the purpose of conciseness the definitions of some functions in the second section are listed here.

$$A_{j\rm imn}^{(l)}(r_i,\theta_i,\phi_i)=r_j^{-n-1}\left[-mP_n^m(\mu_j)(1-\mu_j^2)^{-1/2}f_{ji}^{(l+3)}\sin(m\phi_j)\right.$$
$$\left.+(1-\mu_j^2)^{1/2}\frac{dP_n^m(\mu_j)}{d\mu_j}f_{ji}^{(l+6)}\cos(m\phi_j)\right] \quad \text{(C1)}$$

$$B_{j\rm imn}^{(l)}(r_i,\theta_i,\phi_i)=r_j^{-n-1}\left[(1-\mu_j^2)^{1/2}\frac{dP_n^m(\mu_j)}{d\mu_j}f_{ji}^{(l+6)}\sin(m\phi_j)\right.$$
$$\left.+mP_n^m(\mu_j)(1-\mu_j^2)^{-1/2}f_{ji}^{(l+3)}\cos(m\phi_j)\right] \quad \text{(C2)}$$

$$C_{j\rm imn}^{(l)}(r_i,\theta_i,\phi_i)=r_j^{-n-2}\left\{-mP_n^m(\mu_j)(1-\mu_j^2)^{-1/2}f_{ji}^{(l+6)}\sin(m\phi_j)\right.$$
$$-\left[(n+1)P_n^m(\mu_j)f_{ji}^{(l)}\right.$$
$$\left.\left.+(1-\mu_j^2)^{1/2}\frac{dP_n^m(\mu_j)}{d\mu_j}f_{ji}^{(l+3)}\right]\cos(m\phi_j)\right\} \quad \text{(C3)}$$

$$D_{j\rm imn}^{(l)}(r_i,\theta_i,\phi_i)=r_j^{-n-2}\left\{-\left[(n+1)P_n^m(\mu_j)f_{ji}^{(l)}+(1-\mu_j^2)^{1/2}\right.\right.$$
$$\left.\times\frac{dP_n^m(\mu_j)}{d\mu_j}f_{ji}^{(l+3)}\right]\sin(m\phi_j)$$
$$\left.+mP_n^m(\mu_j)(1-\mu_j^2)^{-1/2}f_{ji}^{(l+6)}\cos(m\phi_j)\right\} \quad \text{(C4)}$$

$$E_{j\,imn}^{(l)}(r_i,\theta_i,\phi_i)=\frac{r_j^{-n}}{2\eta(2n-1)}\left\{m\,\frac{n-2}{n}\,P_n^m(\mu_j)\,(1-\mu_j^2)^{-1/2}\right.$$

$$\times f_{ji}^{(l+6)}\sin(m\phi_j)+\left[\,(n+1)P_n^m(\mu_j)f_{ji}^{(l)}\right.$$

$$\left.\left.+\frac{n-2}{n}\,(1-\mu_j^2)^{1/2}\,\frac{dP_n^m(\mu_j)}{d\mu_j}\,f_{ji}^{(l+3)}\right]\cos(m\phi_j)\right\}\tag{C5}$$

$$F_{j\,imn}^{(l)}(r_i,\theta_i,\phi_i)=\frac{r_j^{-n}}{2\eta(2n-1)}\left\{\left[\,(n+1)P_n^m(\mu_j)f_{ji}^{(l)}\right.\right.$$

$$\left.+\frac{n-2}{n}\,(1-\mu_j^2)^{1/2}\,\frac{dP_n^m(\mu_j)}{d\mu_j}\,f_{ji}^{(l+3)}\right]\sin(m\phi_j)$$

$$\left.-m\,\frac{n-2}{n}\,P_n^m(\mu_j)\,(1-\mu_j^2)^{-1/2}f_{ji}^{(l+6)}\cos(m\phi_j)\right\}.\tag{C6}$$

In Eqs. C1 to C6, $l=1$, 2, and 3, $f_{ji}^{(1)}$, $f_{ji}^{(2)}$, $\ldots$, and $f_{ji}^{(9)}$ are defined by Eqs. 9, and the coordinates (r_j,μ_j,ϕ_j) of an arbitrary point relative to the jth sphere are related to the coordinates (r_i,μ_i,ϕ_i) of the point relative to the ith sphere by Eqs. 7.

$$B_n'(r_i,u_i)=-r_j^{-n-1}P_n^1(u_j)\,(1-u_j^2)^{-1/2}f_{ji2}\tag{C7}$$

$$C_n'(r_i,u_i)=-r_j^{-n-2}\left[\,(n+1)P_n^1(u_j)f_{ji1}-(1-u_j^2)^{1/2}\,\frac{dP_n(u_j)}{du_j}\,f_{ji2}\right]\tag{C8}$$

$$E_n'(r_i,\mu_i)=\frac{r_j^{-n}}{2\eta(2n-1)}\left[(n+1)P_n^1(u_j)f_{ji1}-\frac{(n-2)}{n}\,(1-u_j^2)^{1/2}\,\frac{dP_n^1(u_j)}{du_j}\,f_{ji2}\right]\tag{C9}$$

$$B_n''(r_i,u_i)=r_j^{-n-1}P_n^1(u_j)\,(1-u_j^2)^{-1/2}f_{ji1}\tag{C10}$$

$$C_n''(r_i,u_i)=-r_j^{-n-2}\left[\,(n+1)P_n^1(u_j)f_{ji2}+(1-u_j^2)^{1/2}\,\frac{dP_n^1(u_j)}{du_j}\,f_{ji1}\right]\tag{C11}$$

$$E_n''(r_i,u_i)=\frac{r_j^{-n}}{2\eta(2n-1)}\left[(n+1)P_n^1(u_j)f_{ji2}+\frac{(n-2)}{n}\,(1-u_j^2)^{1/2}\,\frac{dP_n^1(u_j)}{du_j}\,f_{ji1}\right]\tag{C12}$$

$$B_n'''(r_i,u_i)=r_j^{-n-1}(1-u_j^2)^{1/2}\,\frac{dP_n^1(u_j)}{du_j}\tag{C13}$$

$$C_n'''(r_i,u_i)=-r_j^{-n-2}(1-u_j^2)^{-1/2}P_n^1(u_j)\tag{C14}$$

$$E_n'''(r_i,u_i)=\frac{r_j^{-n}}{2\eta(2n-1)}\,\frac{(n-2)}{n}\,(1-u_j^2)^{-1/2}P_n^1(u_j);\tag{C15}$$

$$B_n^*(r_i,u_i)=-(n+1)r_j^{-n-2}\,\frac{\partial r_j}{\partial r_i}\,[P_n^1(u_j)\,(1-u_j^2)^{-1/2}f_{ji1}]$$

$$+r_j^{-n-1}\left[P_n^1(u_j)\,(1-u_j^2)^{-1/2}\,\frac{\partial f_{ji1}}{\partial r_i}-f_{ji1}\,\frac{dP_n^1(u_j)}{du_j}\,\frac{\partial\theta_j}{\partial r_i}-(1-u_j^2)^{-1}u_jP_n^1(u_j)f_{ji1}\,\frac{\partial\theta_j}{\partial r_i}\right]$$

$$+a_i^{-1}\left\{(n+1)r_j^{-n-2}\,\frac{\partial r_j}{\partial\theta_i}\,P_n^1(u_j)f_{ji2}(1-u_j^2)^{-1/2}\right.$$

$$+r_j^{-n-1}\left[f_{ji2}\,\frac{dP_n^1(u_j)}{du_j}\,\frac{\partial\theta_j}{\partial\theta_i}-P_n^1(u_j)\,(1-u_j^2)^{-1/2}\,\frac{\partial f_{ji2}}{\partial\theta_i}\right.$$

$$\left.\left.+(1-u_j^2)^{-1}u_jP_n^1(u_j)f_{ji2}\,\frac{\partial\theta_j}{\partial\theta_i}\right]-B_n''(r_i,u_i)\right\}\tag{C16}$$

$$C_n^*(r_i,u_i)=(n+2)r_j^{-n-3}\,\frac{\partial r_j}{\partial r_i}\left[\,(n+1)P_n^1(u_j)f_{ji2}+(1-u_j^2)^{1/2}\,\frac{dP_n^1(u_j)}{du_j}\,f_{ji1}\right]$$

$$+r_j^{-n-2}\left[\,(n+1)f_{ji2}(1-u_j^2)^{1/2}\,\frac{dP_n^1(u_j)}{du_j}\,\frac{\partial\theta_j}{\partial r_i}-(n+1)P_n^1(u_j)\,\frac{\partial f_{ji2}}{\partial r_i}\right.$$

$$+u_j\,\frac{dP_n^1(u_j)}{du_j}\,f_{ji1}\,\frac{\partial\theta_j}{\partial r_i}-(1-u_j^2)^{1/2}\,\frac{dP_n^1(u_j)}{du_j}\,\frac{\partial f_{ji2}}{\partial r_i}$$

$$\left.+(1-u_j^2)\,\frac{d}{du_j}\left(\frac{dP_n^1(u_j)}{du_j}\right)f_{ji1}\,\frac{\partial\theta_j}{\partial r_i}\right]$$

$$+a_i^{-1}\left\{(n+2)r_j^{-n-3}\,\frac{\partial r_j}{\partial\theta_i}\left[\,(n+1)P_n^1(\mu_j)f_{ji1}-(1-u_j^2)^{1/2}\,\frac{dP_n^1(u_j)}{du_j}\,f_{ji2}\right]\right.$$

$$+r_j^{-n-2}\left[\,(n+1)f_{ji1}(1-u_j^2)^{1/2}\,\frac{dP_n^1(u_j)}{du_j}\,\frac{\partial\theta_j}{\partial\theta_i}-(n+1)P_n^1(u_j)\,\frac{\partial f_{ji1}}{\partial\theta_i}\right.$$

$$+u_j\,\frac{dP_n^1(u_j)}{du_j}\,f_{ji2}\,\frac{\partial\theta_j}{\partial\theta_i}+(1-u_j^2)^{1/2}\,\frac{dP_n^1(u_j)}{du_j}\,\frac{\partial f_{ji2}}{\partial\theta_i}$$

$$\left.\left.-(1-u_j^2)\,\frac{d}{du_j}\left(\frac{dP_n^1(u_j)}{du_j}\right)f_{ji2}\,\frac{\partial\theta_j}{\partial r_i}\right]-B_n''(r_i,u_i)\right\}\tag{C17}$$

$$E_n^*(r_i,u_i)=\frac{1}{2\eta(2n-1)}\left\{-nr_j^{-n-1}\,\frac{\partial r_j}{\partial r_i}\left[\,(n+1)P_n^1(u_j)f_{ji2}+\frac{(n-2)}{n}\,(1-u_j^2)^{1/2}\,\frac{dP_n^1(u_j)}{du_j}\,f_{ji1}\right]+r_j^{-n}\left[\,(n+1)P_n^1(u_j)\,\frac{\partial f_{ji2}}{\partial r_i}\right.\right.$$

$$-(n+1)f_{ji2}(1-u_j^2)^{1/2}\,\frac{dP_n^1(u_j)}{du_j}\,\frac{\partial\theta_j}{\partial r_i}+\frac{(n-2)}{n}\,u_j\,\frac{dP_n^1(u_j)}{du_j}\,f_{ji1}\,\frac{\partial\theta_j}{\partial r_i}$$

$$+\frac{(n-2)}{n}\,(1-u_j^2)^{1/2}\,\frac{dP_n^1(u_j)}{du_j}\,\frac{\partial f_{ji1}}{\partial r_i}$$

$$\left.-\frac{(n-2)}{n}\,(1-u_j^2)\,\frac{d}{du_j}\left(\frac{dP_n^1(u_j)}{du_j}\right)f_{ji1}\,\frac{\partial\theta_j}{\partial r_i}\right]$$

$$+a_i^{-1}\left\{nr_j^{-n-1}\frac{\partial r_j}{\partial\theta_i}\left[\frac{(n-2)}{n}(1-u_j^2)^{1/2}\frac{dP_n^1(u_j)}{du_j}f_{ji2}\right.\right.$$

$$\left.-(n+1)P_n^1(u_j)f_{ji1}\right]+r_j^{-n}\left[(n+1)P_n^1(u_j)\frac{\partial f_{ji1}}{\partial\theta_i}\right.$$

$$-(n+1)f_{ji1}(1-u_j^2)^{1/2}\frac{dP_n^1(u_j)}{du_j}\frac{\partial\theta_j}{\partial\theta_i}-\frac{(n-2)}{n}u_j\frac{\partial\theta_j}{\partial\theta_i}\frac{dP_n^1(u_j)}{du_j}f_{ji2}$$

$$-\frac{(n-2)}{n}(1-u_j^2)^{1/2}\frac{dP_n^1(u_j)}{du_j}\frac{\partial f_{ji2}}{\partial\theta_i}+\frac{(n-2)}{n}(1-u_j^2)$$

$$\left.\left.\times\frac{d}{du_j}\left(\frac{dP_n^1(u_j)}{du_j}\right)f_{ji2}\frac{\partial\theta_j}{\partial\theta_i}\right]\right\}-a_i^{-1}E_n''(r_i,u_i)\quad\text{(C18)}$$

$$B_n^{**}(r_i,u_i)=-(n+1)r_j^{-n-2}\frac{\partial r_j}{\partial r_i}(1-u_j^2)^{1/2}\frac{dP_n^1(u_j)}{du_j}$$

$$+r_j^{-n-1}\frac{\partial\theta_j}{\partial r_i}\left[u_j\frac{dP_n^1(u_j)}{du_j}-(1-u_j^2)\frac{d}{du_j}\left(\frac{dP_n^1(u_j)}{du_j}\right)\right]$$

$$-a_i^{-1}B_n'''(r_i,u_i)-a_i^{-1}(1-u_i^2)^{-1/2}B_n'(r_i,u_i)\quad\text{(C19)}$$

$$C_n^{**}(r_i,u_i)=(n+2)r_j^{-n-3}\frac{\partial r_j}{\partial r_i}P_n^1(u_j)(1-u_j^2)^{-1/2}$$

$$+r_j^{-n-2}\frac{\partial\theta_j}{\partial r_i}\left[(1-u_j^2)^{-1}u_jP_n^1(u_j)+\frac{dP_n^1(u_j)}{du_j}\right]$$

$$-a_i^{-1}C_n'''(r_i,u_i)-a_i^{-1}(1-u_i^2)^{-1/2}C_n'(r_i,u_i)\quad\text{(C20)}$$

$$E_n^{**}(r_i,u_i)=\frac{(2-n)}{2\eta_i(2n-1)}\left\{r_j^{-n-1}\frac{\partial r_j}{\partial r_i}P_n^1(u_j)(1-u_j^2)^{-1/2}\right.$$

$$\left.+\frac{1}{n}r_j^{-n}\frac{\partial\theta_j}{\partial r_i}\left[(1-u_j^2)^{-1}u_jP_n^1(u_j)-\frac{dP_n^1(u_j)}{du_j}\right]\right\}$$

$$-a_i^{-1}E_n'''(r_i,u_i)-a_i^{-1}(1-u_i^2)^{-1/2}E_n'(r_i,u_i).\quad\text{(C21)}$$

In Eqs. C7 to C21,

$$f_{ji1}=(1-u_j^2)^{1/2}(1-u_i^2)^{1/2}+u_ju_i\quad\text{(C22)}$$

$$f_{ji2}=(1-u_j^2)^{1/2}u_i-u_j(1-u_i^2)^{1/2};\quad\text{(C23)}$$

$$\frac{\partial r_j}{\partial r_i}=(r_i+u_id_{ji})/r_j\quad\text{(C24)}$$

$$\frac{\partial\theta_j}{\partial r_i}=\left[\frac{\partial r_j}{\partial r_i}(r_iu_i+d_{ji})-u_ir_j\right](1-u_j^2)^{-1/2}/r_j^2\quad\text{(C25)}$$

$$\frac{\partial r_j}{\partial\theta_i}=-r_i(1-u_i^2)^{1/2}d_{ji}/r_j\quad\text{(C26)}$$

$$\frac{\partial\theta_j}{\partial\theta_i}=\left[\frac{\partial r_j}{\partial\theta_i}(r_iu_i+d_{ji})+r_ir_j(1-u_i^2)^{1/2}\right](1-u_j^2)^{-1/2}/r_j^2\quad\text{(C27)}$$

$$\frac{\partial f_{ji2}}{\partial\theta_i}=-[u_ju_i+(1-u_j^2)^{1/2}(1-u_i^2)^{1/2}]\left(1-\frac{\partial\theta_j}{\partial\theta_i}\right)\quad\text{(C28)}$$

$$\frac{\partial f_{ji1}}{\partial\theta_i}=[u_i(1-u_j^2)^{1/2}-u_j(1-u_i^2)^{1/2}]\left(1-\frac{\partial\theta_j}{\partial\theta_i}\right)\quad\text{(C29)}$$

$$\frac{\partial f_{ji1}}{\partial r_i}=[u_j(1-u_i^2)^{1/2}-u_i(1-u_j^2)^{1/2}]\frac{\partial\theta_j}{\partial r_i}\quad\text{(C30)}$$

$$\frac{\partial f_{ji2}}{\partial r_i}=[u_ju_i+(1+u_j^2)^{1/2}(1-u_i^2)^{1/2}]\frac{\partial\theta_j}{\partial r_i}.\quad\text{(C31)}$$

Notation

a = radius of droplet, m
a_i = radius of droplet i, m
$A_{jmn}, B_{jmn}, C_{jmn}$ $\underline{D}_{jmn}, \underline{E}_{jmn}, \underline{F}_{jmn}$ = coefficients in the expression of Eq. 6a for the external flow field
$\bar{A}_{imn}, \bar{B}_{imn}, \bar{C}_{imn}$, $\bar{D}_{imn}, \bar{E}_{imn}, \bar{F}_{imn}$ = coefficients in the expression of Eq. 6b for the flow field inside droplet i
$A_{jimn}^{(l)}, B_{jimn}^{(l)}, C_{jimn}^{(l)}$, $D_{jimn}^{(l)}, E_{jimn}^{(l)}, F_{jimn}^{(l)}$ = functions of r_i, θ_i and ϕ_i defined by Eqs. C1 to C6
$B_{jin}', C_{jin}', E_{jin}'$, $B_{jin}'', C_{jin}'', E_{jin}''$ $B_{jin}''', C_{jin}''', E_{jin}'''$, = functions of r_i and μ_i defined by Eqs. C7 to C15
$B_{jin}^{*}, C_{jin}^{*}, E_{jin}^{*}$, $B_{jin}^{**}, C_{jin}^{**}, E_{jin}^{**}$ = functions of r_i and μ_i defined by Eqs. C16 to C21
b_i, c_i, d_i = rectangular coordinates of the center of droplet i, m
b_{ij}, c_{ij}, d_{ij} = equal to b_i-b_j, c_i-c_j, d_i-d_j, respectively, m
d = distance between the centers of two neighboring droplets in a chain of equally spaced identical droplets, m
$\underline{e}_x, \underline{e}_y, \underline{e}_z$ = unit vectors in rectangular coordinates
$\underline{e}_{ri}, \underline{e}_{\theta i}, \underline{e}_{\phi i}$ = unit vectors in the spherical coordinates originated from droplet i
$f_{ji}^{(l)}$ = coefficients for the transformation of unit vectors in two spherical coordinates defined by Eqs. 9
$\underline{F}_i, F_i$ = drag force acting on droplet i, N
$\underline{F}_j^{(0)}$ = drag force acting on droplet j in the absence of all the other droplets, N
$G_n^{-1/2}$ = the Gegenbauer polynomial of order n and degree $-1/2$
$\underline{\underline{I}}$ = unit dyadic
K = the number of collocation rings on each droplet interface
$\underline{\underline{K}}_{ij}$ = dimensionless resistance tensors defined by Eq. 17 or B6a
$K_{ij}^{(p)}, K_{ij}^{(n)}$ = dimensionless resistance parameters defined by Eq. 24
m_j = mobility of droplet j defined by Eq. 19, $s\cdot kg^{-1}$
M = the number of terms reserved in the Fourier series
$\underline{\underline{M}}_{ij}$ = dimensionless mobility tensors defined by Eq. 21 or B9a
$M_{ij}^{(p)}, M_{ij}^{(n)}$ = dimensionless mobility parameters defined by Eq. 25
N = the number of droplets in an assemblage
$\underline{\underline{N}}_{ij}, \underline{\underline{Q}}_{ij}, \bar{\underline{\underline{Q}}}_{ij}$ = dimensionless mobility tensors defined by Eqs. B9
p = pressure distribution of the external fluid, $N\cdot m^{-2}$
p_i = pressure distribution inside droplet i, $N\cdot m^{-2}$
P_n = the Legendre polynomial of order n
P_n^m = the associated Legendre function of order m and degree n

$\underline{\underline{P}}_{ij}$, $\overline{\underline{\underline{P}}}_{ij}$, $\underline{\underline{R}}_{ij}$ = dimensionless resistance tensors defined by Eq. B6
Q_{ij} = dimensionless rotational mobility parameters defined by Eq. 28
r, θ, ϕ = spherical coordinates
r_i, θ_i, ϕ_i = spherical coordinates measured from the origin of droplet i
$\underline{r}_i$ = position vector in spherical coordinates (r_i, θ_i, ϕ_i), m
r_{ji} = distance between the centers of the jth and ith droplets, m
$\underline{T}_i$ = hydrodynamic torque on sphere i about its center, N·m
$\underline{T}_j^{(0)}$ = hydrodynamic torque on sphere j in the absence of all the other spheres, N·m
$\underline{U}_i$ = translational velocity of droplet i, $m \cdot s^{-1}$
U_{ix}, U_{iy}, U_{iz} = components of $\underline{U}_i$ in rectangular coordinates, $m \cdot s^{-1}$
$\underline{U}_j^{(0)}$ = translational velocity of droplet j in the absence of all the other spheres, $m \cdot s^{-1}$
$\langle \underline{U}_i \rangle$ = mean settling velocity of type i droplets, $m \cdot s^{-1}$
$\underline{v}$ = velocity field of the external fluid, $m \cdot s^{-1}$
$\underline{v}_i$ = velocity field inside droplet i, $m \cdot s^{-1}$
v_r, v_θ, v_ϕ = components of $\underline{v}$ in spherical coordinates (r_i, θ_i, ϕ_i), $m \cdot s^{-1}$
$v_{ri}, v_{\theta i}, v_{\phi i}$ = components of $\underline{v}_i$ in spherical coordinates (r_i, θ_i, ϕ_i), $m \cdot s^{-1}$
v_ρ, v_z = velocity components of the external fluid in cylindrical coordinates, $m \cdot s^{-1}$
$v_{i\rho}, v_{iz}$ = velocity components of the fluid inside droplet i in cylindrical coordinates, $m \cdot s^{-1}$
x, y, z = rectangular coordinates, m

Greek letters

α_{in}, γ_{in} = coefficients in the expression of Eq. A4b for the axisymmetric flow field inside droplet i
$\alpha_n', \gamma_n', \alpha_n'', \gamma_n''$ = functions of r_i and μ_i defined by Eqs. A7e to A7h
α_n^*, γ_n^* = functions of r_i and μ_i defined by Eqs. A10e to A10f
β_{jn}, δ_{jn} = coefficients in the expression of Eq. A4a for the axisymmetric external flow field
$\beta_n', \delta_n', \beta_n'', \delta_n''$ = functions of r_j and μ_j defined by Eqs. A7a to A7d
$\beta_n^*, \delta_n^*, \beta_n^{**}, \delta_n^{**}$ = functions of r_j and μ_j defined by Eqs. A10a to A10d
γ_i = interfacial tension at the interface of droplet i, $N \cdot m^{-1}$
η = viscosity of the external fluid, $kg \cdot m^{-1} \cdot s^{-1}$
η_i = viscosity of the fluid inside droplet i, $kg \cdot m^{-1} \cdot s^{-1}$
η^* = ratio of viscosity between the internal and surrounding fluids
η_i^* = η_i/η
λ = viscosity parameter defined by Eq. 33
μ_i = $\cos\theta_i$
ν_{ij} = interaction coefficient defined by Eq. 30
ρ, ϕ, z = circular cylindrical coordinates
$\underline{\underline{\tau}}$ = viscous stress tensor of the external fluid, $kg \cdot m^{-1} \cdot s^{-2}$
$\underline{\underline{\tau}}_i$ = viscous stress tensor of the fluid inside droplet i, $kg \cdot m^{-1} \cdot s^{-2}$
$\chi_n^{(i)}, \phi_n^{(i)}, p_n^{(i)}$ = solid spherical harmonic functions of order n in spherical coordinates (r_i, θ_i, ϕ_i)
φ_i = volume fraction of type i droplets in a suspension
Ψ = the Stokes stream function of the external fluid, $m^3 \cdot s^{-1}$
Ψ_i = the Stokes stream function of the fluid inside droplet i, $m^3 \cdot s^{-1}$
ω = separation parameter defined by Eq. 34
$\underline{\Omega}_i$ = angular velocity of sphere i, s^{-1}
$\Omega_{ix}, \Omega_{iy}, \Omega_{iz}$ = components of $\underline{\Omega}_i$ in rectangular coordinates, s^{-1}
$\underline{\Omega}_j^{(0)}$ = angular velocity of sphere j in the absence of all the other spheres, s^{-1}

Literature Cited

Bart, E., "The Slow Unsteady Settling of a Fluid Sphere toward a Flat Fluid Interface," *Chem. Eng. Sci.*, **23**, 193 (1968).

Batchelor, G. K., "Sedimentation in a Dilute Dispersion of Spheres," *J. Fluid Mech.*, **52**, 245 (1972).

Brenner, H., "The Slow Motion of a Sphere through a Viscous Fluid towards a Plane Surface," *Chem. Eng. Sci.*, **16**, 242 (1961).

Brenner, H., "Pressure Drop Due to the Motion of Neutrally Buoyant Particles in Duct Flows. II. Spherical Droplets and Bubbles," *Ind. Eng. Chem. Fund.*, **10**, 537 (1971).

Cooley, M. D. A., and M. E. O'Neill, "On the Slow Motion of Two Spheres in Contact along Their Line of Centres through a Viscous Fluid," *Proc. Comb. Phil. Soc.*, **66**, 407 (1969).

Coutanceau, M., and P. Thizon, "Wall Effect on the Bubble Behaviour in Highly Viscous Liquids," *J. Fluid Mech.*, **107**, 339 (1981).

Dandy, D. S., and L. G. Leal, "Buoyancy-Driven Motion of a Deformable Drop through a Quiescent Liquid at Intermediate Reynolds Numbers," *J. Fluid Mech.*, **208**, 161 (1989).

Davis, M. H., "The Slow Translation and Rotation of Two Unequal Spheres in a Viscous Fluid," *Chem. Eng. Sci.*, **24**, 1769 (1969).

Davis, R. H., J. A. Schonberg, and J. M. Rallison, "The Lubrication Force between Two Viscous Drops," *Phys. Fluids A*, **1**, 77 (1989).

Fuentes, Y. O., S. Kim, and D. J. Jeffrey, "Mobility Functions for Two Unequal Viscous Drops in Stokes Flow. I. Axisymmetric Motions," *Phys. Fluids*, **31**, 2445 (1988).

Fuentes, Y. O., S. Kim, and D. J. Jeffrey, "Mobility Functions for Two Unequal Viscous Drops in Stokes Flow. II. Asymmetric Motions," *Phys. Fluids A*, **1**, 61 (1989).

Ganatos, P., R. Pfeffer, and S. Weinbaum, "A Numerical-Solution Technique for Three-Dimensional Stokes Flows, with Application to the Motion of Strongly Interacting Spheres in a Plane," *J. Fluid Mech.*, **84**, 79 (1978).

Geigenmuller, U., and P. Mazur, "Many-Body Hydrodynamic Interactions between Spherical Drops in an Emulsion," *Physica A*, **138**, 269 (1986).

Gerald, C. F., and P. O. Wheatley, "Applied Numerical Analysis," p. 106, 4th ed., Addison-Wesley, Reading, MA (1989).

Gluckman, M. J., R. Pfeffer, and S. Weinbaum, "A New Technique for Treating Multiparticle Slow Viscous Flow: Axisymmetric Flow Past Spheres and Spheroids," *J. Fluid Mech.*, **50**, 705 (1971).

Goldman, A. J., R. G. Cox, and H. Brenner, "The Slow Motion of Two Identical Arbitrarily Oriented Spheres through a Viscous Fluid," *Chem. Eng. Sci.*, **21**, 1151 (1966).

Haber, S., and G. Hetsroni, "Sedimentation in a Dilute Dispersion of Small Drops of Various Sizes," *J. Colloid Interface Sci.*, **79**, 56 (1981).

Haber, S., G. Hetsroni, and A. Solan, "On the Low Reynolds Number Motion of Two Droplets," *Int. J. Multiphase Flow*, **1**, 57 (1973).

Hadamard, J. S., "Mouvement Permanent Lent d'Une Sphere Liquide et Visqueuse dans Un Liquide Visqueux," *Compt. Rend. Acad. Sci. (Paris)*, **152**, 1735 (1911).

Happel, J., and H. Brenner, "Low Reynolds Number Hydrodynamics," Martinus Nijhoff, The Netherlands (1983).

Hassonjee, Q., P. Ganatos, and R. Pfeffer, "A Strong-Interaction Theory for the Motion of Arbitrary Three-Dimensional Clusters of Spherical Particles at Low Reynolds Number," *J. Fluid Mech.*, **197**, 1 (1988).

Hetsroni, G., and S. Haber, "Low Reynolds Number Motion of Two Drops Submerged in an Unbounded Arbitrary Velocity Field," *Int. J. Multiphase Flow*, **4**, 1 (1978).

Hetsroni, G., S. Haber, and E. Wacholder, "The Flow Fields in and around a Droplet Moving Axially within a Tube," *J. Fluid Mech.*, **41**, 689 (1970).

Jeffrey, D. J., and Y. Onishi, "Calculation of the Resistance and Mobility Functions for Two Unequal Rigid Spheres in Low-Reynolds-Number Flow," *J. Fluid Mech.*, **139**, 261 (1984).

Keh, H. J., and F. R. Yang, "Particle Interactions in Electrophoresis. IV. Motion of Arbitrary Three-Dimensional Clusters of Spheres," *J. Colloid Interface Sci.*, **145**, 362 (1991).

Kim, S., and S. J. Karrila, "Microhydrodynamics: Principles and Selected Applications," p. 237, Butterworth-Heinemann, Boston (1991).

Maude, A. D., "End Effects in a Falling-Sphere Viscometer," *Brit. J. Appl. Phys.*, **12**, 293 (1961).

O'Brien, V., "Form Factors for Deformed Spheroids in Stokes Flow," *AIChE J.*, **14**, 870 (1968).

Reed, C. C., and J. L. Anderson, "Hindered Settling of a Suspension at Low Reynolds Number," *AIChE J.*, **26**, 816 (1980).

Reed, L. D., and F. A. Morrison, "The Slow Motion of Two Touching Fluid Spheres along Their Line of Centers," *Int. J. Multiphase Flow*, **1**, 573 (1974).

Rushton, E., and G. A. Davies, "The Slow Unsteady Settling of Two Fluid Spheres along Their Line of Centres," *Appl. Sci. Res.*, **28**, 37 (1973).

Rushton, E., and G. A. Davies, "The Slow Motion of Two Spherical Particles along Their Line of Centres," *Int. J. Multiphase Flow*, **4**, 357 (1978).

Rybczynski, W., "Uber die Fortschreitende Bewegung Einer Flussigen Kugel in Einem Zahen Medium," *Bull. Acad. Sci. Cracovie* (*Ser. A*), **40** (1911).

Shapira, M., and S. Haber, "Low Reynolds Number Motion of a Droplet between Two Parallel Plates," *Int. J. Multiphase Flow*, **14**, 483 (1988).

Stimson, M., and G. B. Jeffery, "The Motion of Two Spheres in a Viscous Fluid," *Proc. Roy. Soc., A*, **111**, 110 (1926).

Taylor, T. D., and A. Acrivos, "On the Deformation and Drag of a Falling Viscous Drop at Low Reynolds Number," *J. Fluid Mech.*, **18**, 466 (1964).

Wacholder, E., and D. Weihs, "Slow Motion of a Fluid Sphere in the Vicinity of Another Sphere or a Plane Boundary," *Chem. Eng. Sci.*, **27**, 1817 (1972).

Manuscript received March 3, 1992, and revision received June 17, 1992.